Fuel 303 (2021) 121327

Contents lists available at ScienceDirect

Fuel

journal homepage: www.elsevier.com/locate/fuel

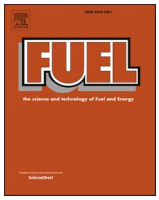

Full Length Article

Analysis and selection of optimal solvent-based technologies for biogas upgrading

Andrés Carranza-Abaid *, Ricardo R. Wanderley, Hanna K. Knuutila, Jana Poplsteinova Jakobsen

Department of Chemical Engineering, Norwegian University of Science and Technology (NTNU), NO-7491 Trondheim, Norway

ARTICLE INFO

Keywords:
Biogas upgrading
CO_2 capture
Chemical absorption
Physical absorption

ABSTRACT

Biogas upgrading is an important industrial process for producing biomethane, a sustainable energy source with low carbon footprint. There are three main solvent-based alternatives for biogas upgrading: water scrubbing, physical scrubbing and chemical scrubbing with amines. Though assessments have been published regarding which technologies are more cost-effective and energetically efficient, these often either neglect inspecting the impact of raw biogas concentrations and biomethane delivery pressures on the overall performance of the plant, or they do not consider that the separated CO_2 has to be conditioned for transportation for properly fulfilling the requirements of BECCS (bioenergy with carbon capture and storage). In fact, many assessments of physical scrubbing processes forfeit CO_2 recovery altogether. This work intends to rehabilitate physical scrubbing as an alternative for BECCS by showing that, depending on the conditions of the raw biogas, the requirements for biomethane delivery, and the cost of carbon taxes, biogas upgrading can be feasible by scrubbing either with amines or with organic solvents. We introduce a review on organic physical solvents for CO_2 recovery, a simulation framework for the evaluation of energetical operational costs of biogas upgrading, and a simplified economic analysis. High biomethane delivery pressures and high CO_2 concentrations in raw biogas benefit the use of physical solvents such as N-formyl-morpholine, N-methyl-2-pyrrolidone and poly(ethylene glycol) dimethyl ether, whereas the opposite conditions are advantageous to aqueous monoethanolamine. Finally, the implementation of carbon taxes of around 10 USD/ton CO_2 emitted are sufficient to increase the attractiveness of CO_2 recovery as opposed to CO_2 wasting.

1. Introduction

In past decades, the development of sustainable energy generation technologies has become an important asset in mitigating climate change and environmental degradation. These include technologies such as improved solar panels, efficient wind-powered equipment, hydrogen fuel cells and biogas production facilities [1]. Of these, biogas production can be inserted in the wider context of negative emissions [2] and, therefore, deserves a careful assessment.

Biogas is a mixture containing mostly methane (CH_4, 40–75 %v/v) and carbon dioxide (CO_2) [3], with typical secondary impurities being hydrogen sulfide (H_2S), ammonia (NH_3), siloxanes, halogenates and volatile organic carbon (VOC) compounds such as ketones, alkanes and terpenes [3–6]. *Biogas upgrading* is the name given to the process of removing CO_2 from raw biogas. Since biogas is produced biologically through anaerobic digestion of organic matter, both the nature of the digestate and the conditions of the biological fermentation will affect the composition of raw biogas [6–8]. This is of interest to the industry, since this raw biogas must often be treated before it is delivered as high purity biomethane, and the degree of complexity required for this treatment naturally impacts the sort of technologies needed to perform the task [3,4,6]. There are numerous biogas producing plants that include a biogas upgrading process [9].

Utilization of biogas through combustion inevitably generates CO_2 and cannot be strictly considered a green energy alternative. However, if biogas is produced from a biomass source that participates in a stable carbon cycle (i.e., in which the production of biomass by plants or algae consuming atmospheric CO_2 happens at rate comparable to that of combustion of the resulting biogas), then the net amount of CO_2 emitted at the end of such cycle can be said to approach zero [10]. Surely enough, assuring that a process is “net-zero” is a delicate matter which requires careful evaluation of all of its intermediary steps. One practical

* Corresponding author.
E-mail address: andres.c.abaid@ntnu.no (A. Carranza-Abaid).

https://doi.org/10.1016/j.fuel.2021.121327
Received 3 March 2021; Received in revised form 17 June 2021; Accepted 21 June 2021

way of reducing the odds of having a disbalanced biogas production cycle is by capturing part of the CO_2 that is generated together with biomethane before delivering the latter to its final user. Then, the technology can be said to have achieved *negative emissions*: part of the CO_2 utilized for biomass production in the beginning of the process ends up removed from the carbon cycle through CCS (*carbon capture and storage*) alternatives [2,11].

This is an important facet of the so-called BECCS (*bioenergy with CCS*): from an environmental perspective, the process of biogas upgrading together with CO_2 recovery is not only practical for the consumer (e.g., to generate a stream with higher heating value), but it is also indispensable towards achieving negative emissions in the industry. In this aspect, biogas upgrading *without* CO_2 recovery – i.e., removing CO_2 from raw biogas and then emitting it to the atmosphere – is a practice that should be ultimately discouraged.

One of the several policies suggested in the Paris agreement in order to achieve the global zero greenhouse gas emissions target by 2050 is the implementation of CO_2 taxes. These taxes force companies or production plants to pay a fee for each ton of CO_2 emitted into the atmosphere. Since biogas upgrading plants *may* or *may not* emit the removed CO_2 to the atmosphere, and since carbon taxes *may* or *may not* apply to bioenergy-based plants, the inclusion of these taxes in economic assessments is an uncertainty expected to hold a crucial role in process feasibility, thus reflecting on the optimal CO_2 capture technology for each scenario.

In order to assess this uncertainty, the present study considers the feasibility of biomethane production plants both in the scenario in which they must pay for their CO_2 emissions and in the scenario where this is not a requirement. This may vary depending on the CO_2 emissions policies of the country where the plant is located (see Section 3 for further discussion). We suggest that the performance of different biogas upgrading technologies and the selection of the optimal alternative will change as a function of the following external conditions: the raw biogas properties, the treated biomethane specifications and the value of the CO_2 tax. Our intention is, therefore, to evaluate how these external conditions will impact the choice of a proper upgrading technology.

Ultimately, we repeat, biogas upgrading with CO_2 recovery is environmentally beneficial even when not economically so. It is our goal to identify which upgrading technologies are able to better align financial and environmental considerations by minimizing the cost of BECCS.

This work focuses on solvent-based solutions (i.e., absorption by physical and chemical means) due to their prominence in the biogas upgrading market. We present:

- **BACKGROUND (Section 2).** A summary of biogas upgrading alternatives (Section 2.1), followed by a review of physical (Section 2.2) and chemical (Section 2.3) solvents for CO_2 separation. Though Sections 2.1 and 2.3 are rather cursory, we went into great lengths to make Section 2.2 a proper comprehensive review of physical solvents for CO_2 absorption since we have identified a lack of such a source in the available published literature.
- **PROCESS MODELLING (Section 3).** A methodical explanation of our approach to solvent performance evaluation. Though we employ this approach in the assessment of BECCS in the present study, there is nothing deterring anyone of using such a methodology in the evaluation of other solvent-based processes in different contexts. Hence, we consider that Section 3 in itself can be valuable for future researchers.
- **RESULTS AND DISCUSSION (Section 4).** An energy analysis and an operative-cost-oriented assessment of the economic performance of 4 different technologies: **P**hysical/**W**ater absorption without CO_2 recovery (PW), **P**hysical/**W**ater absorption with **CO_2 R**ecovery (PWCR) (both on Section 4.1), **A**queous a**M**ine chemical absorption without CO_2 recovery (AM) and **A**queous a**M**ine chemical absorption with **CO_2 R**ecovery (AMCR) (both on Section 4.2). This includes an evaluation of different physical solvents, in particular with regards to PWCR (Section 4.1). Additionally, we report an easy-to-use guide on optimal process selection as a function of raw biogas conditions and biomethane delivery pressure. As we present results *with* and *without* the inclusion of carbon taxes, Section 4 is insightful even in the context where there are no penalties for the emission of CO_2 by biogas upgrading plants.

Therefore, the middle bulk of this article contains three very distinct albeit interlinked sections, two laying down important groundwork and one delivering our main results. These sections can be read by themselves, hence we recommend that readers who are interested merely in the outcome of our energetic analysis skip directly to Section 4 and then to Section 5 (the Conclusions). However, we hope to have showed with the table of contents above that each section has its individual value, and that they all contribute to a proper understanding of our results.

2. Background

2.1. Biogas upgrading technologies

There are currently six main biogas upgrading technologies. These are:

- Water scrubbing – using pressurized water to physically absorb CO_2 followed by decompression and/or stripping with an inert gas for regeneration [3,6,8,12] (formerly, the resulting water was just directly wasted as an effluent, but this is generally not acceptable anymore [6,8]).
- Physical scrubbing – similar to water scrubbing, but using an organic solvent instead of water [6,8,13,14]. Solvent regeneration can be of three types: flash desorption (by solvent decompression), stripping with an inert gas, and hot regeneration [15]. More on these organic solvents will be discussed in Section 2.2.
- Chemical scrubbing – a solvent containing a species that chemically reacts with CO_2 is employed for upgrading [4,8,13,14]. This chemical reaction increases the solvent capacity for CO_2 absorption, but also makes regeneration more difficult. Desorption is performed by supplying heat to the system [13,14,16]. More on these chemical solvents will be discussed in Section 2.3.
- Pressure swing adsorption (PSA) – CO_2 is adsorbed over a porous material at high pressures and desorbed at low pressures in the so-called *Skarstrom cycle* [13,17]. The criterium for separation here is the higher CO_2 diffusivity when compared to that of methane (due to its lower molecular size) [6,8,12,14]. Typical materials for CO_2 adsorption are zeolites, silicates, silica gel and activated carbon [8,12], though current research in the field of metal–organic frameworks render these materials particularly attractive.
- Membrane technology – CO_2 is separated from methane due to its lower molecular size in a porous interface using differential partial pressure as the driving force [3,12–14]. Development of such membranes is rapidly advancing [18,19]. For industrial applications, the materials employed are typically polymeric in nature [14], though fast developments might render this information anachronistic.
- Cryogenic separation – CO_2 is condensed at high pressures and low temperatures while methane remains in the gas phase due to the difference between the boiling points [3,6,8]. Due to the high energy-intensity of this process, designing an optimal system configuration is essential, and therein lie most recent advances in this field [20].

Comparisons between these six different techniques can be performed across a variety of criteria, with none being necessarily more or less important than the other. In terms of modularity and flexibility, for example, membranes are commonly argued to be superior to other technologies [21,22] – and yet, they often require an integration of parallel and/or sequential modules to be fully capable of separating CO_2

[18,19], bringing down their energy efficiency [12,14]. Energy consumption is often also high when operating PSA, and its footprint (i.e., the amount of physical space a processing plant occupies) can be problematic [17]. Cryogenic methodologies are expensive both in terms of equipment as well as operational costs, but are able to deliver highly purified biomethane ready for condensation into LBG (*liquid biogas*) together with pressurized CO_2 proper for transportation and storage [8,20]. In terms of robustness to stand impurities, water scrubbing is able to handle most of them easily [12], whereas cryogenic separation can be designed so that each contaminant is removed sequentially according to their relative volatilities [20]. All of the other techniques are vulnerable to one impurity or another, which can devolve in operational issues such as membrane degradation [19] or solvent decomposition [23].

Perhaps the best way to assess the competitiveness of these different technologies is by looking at how they are actually implemented in the biogas upgrading market. Almost every year, IEA Bioenergy publishes a list of the new developed biogas upgrading plants implemented by their member countries (which critically does not include neither China nor the U.S.A.) categorized by chosen upgrading technology. Fig. 1 shows the cumulative number of biogas upgrading plants deployed from 2000 up to 2019 in those member countries. We unfortunately had to ignore the entries in the list for which no installation year was given, but those were very few overall.

Fig. 1 shows a fragmented market between several technologies, with physical scrubbing and cryogenic separation techniques arguably lagging the others. From the perspective of someone coming from either the pre-combustion or post-combustion carbon capture background, this is a somewhat surprising image. In those fields, one typically thinks of chemical absorption as the state-of-the-art CO_2 capture process [24,25]. In the biogas upgrading field, however, chemical scrubbing with amines not only fares poorly compared to membrane technologies, but it is also overshadowed by water scrubbing. Conversely, one finds no instances of water scrubbing ever being used for natural gas treatment nor CO_2 removal from flue gases.

A 2012 study carried by the Vienna University of Technology has come up with a comparison between five of the six technologies mentioned previously, which is summarized on Table 1. Being from 2012, Table 1 is perhaps anachronistic, but its overall message is representative of what has been reported until quite recently regarding biogas upgrading (see [26] for more contemporaneous data). The electrical energy consumption of all different technologies is very similar, with the remarkable exception of chemical scrubbing. This, of course, comes with two caveats. First, chemical scrubbing requires a high thermal energy consumption for its solvent regeneration step, so that looking at electricity consumption alone might be misleading. Second, chemical scrubbing is the technology in which biomethane is delivered at its lowest pressure. As biomethane is most often pressurized for injection into either a medium-pressure (e.g., 16 bars) or high-pressure (e.g., 55 bars) natural gas grid [1], the gas produced by chemical scrubbing is still in need of compression unless it is directly used for energy production. Even with this limitation, however, one can see at the bottom of Table 1 that the operational costs of chemical scrubbing end up above those of the various other technologies.

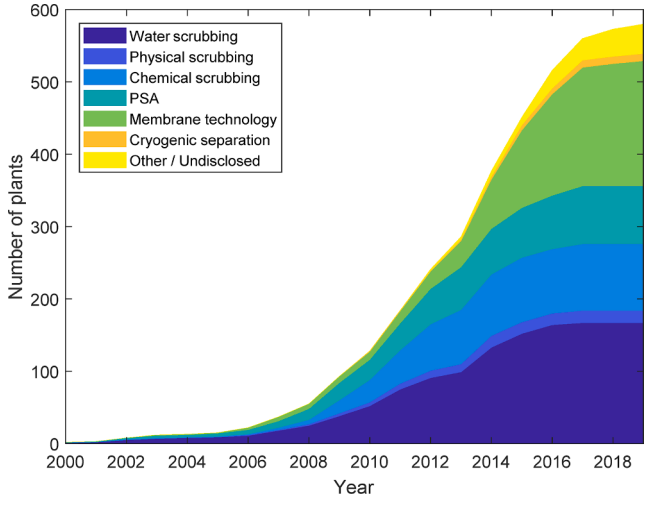

Fig. 1. Cumulative number of biogas upgrading plants installed by IEA Bioenergy member countries divided by their chosen biogas upgrading technologies. List obtained from the IEA Bioenergy website [9].

Table 1
Comparison between biogas upgrading technologies carried by the Vienna University of Technology [32] in 2012. Values typical of plants with a capacity to produce around 500 m^3/h biomethane (average sized biogas upgrading plants).

	Water scrubbing	Physical scrubbing	Chemical scrubbing	PSA	Membrane technology
Biomethane purity (%)	95.0 – 99.0	95.0 – 99.0	>99.0	95.0 – 99.0	95.0 – 99.0
Methane slip (%)	2.0	4.0	0.04	2.0	20.0 – 0.5
Delivery pressure (bar)	5 – 9	5 – 9	1	5 – 8	5 – 8
Electric energy demand (kWh/m^3 biomethane)	0.46	0.49 – 0.67	0.27	0.46	0.25 – 0.43
Heating demand	None	Medium	High	None	None
Typical investment costs (€/m^3/h biomethane)	3500	3500	3500	3700	3500 – 3700
Typical operational costs (€/m^3/h biomethane)	0.091	0.090	0.112	0.092	0.065 – 0.101

Finally, there is something to be said about biomethane purity and methane slip. The demanded biomethane purity is defined by the constraints imposed for its utilization. For biomethane injection into the natural gas grid, the 2016 Deliverable D5.2 from the ISAAC project to the European Commission [27] compiles some of the current national standards: biomethane should contain less than 2.5 %v/v CO_2 in Germany and France, less than 3 %v/v CO_2 in Sweden, Denmark, Austria and the U.K., and less than 6 %v/v in the Netherlands. Though national standards may vary, basic standards for the European Union are given in EN 16723–1 for biomethane injection in the gas grid and in EN 16723–1 for biomethane use in road transport [28] – notice that EU standards do not specify a maximum CO_2 content but a minimum methane number: 65 according to EN 16723–1, 65 or 80 according to EN 16723–2 (depending on fuel grade) [29]. Clearly then, all technologies addressed on Table 1 are capable of producing high quality biomethane. The main difference among processes is methane slip. Other than the obvious loss of profit from reduced productivity, methane slip is an environmental hazard that is typically addressed through regenerative catalytic oxidation (RCO) or regenerative thermal oxidation (RTO) (see the following references [30,31] for a comparison between RCO and RTO), i.e., burning, which involves additional energetic and economic penalties. Chemical scrubbing has a high selectivity for CO_2 separation and consequentially the lowest methane slip values amongst all technologies. The reason for this is the very low solubility of CH_4 into the aqueous amine mixture and the low pressures commonly used in the amine scrubbing processes.

One could then wonder what the most environmentally benign

technology for biogas upgrading is. As it turns out, it depends heavily on the origin of the electricity employed in the biogas upgrading plant [33,34]. This highlights the importance of choosing an energy efficient pathway for biogas upgrading. Therefore, both for deployment considerations and environmental considerations, energy saving is key.

2.2. Physical solvents for CO_2 absorption

In physical scrubbing, the CO_2 binds to the physical solvents by relatively loose intermolecular forces. It has been demonstrated that CO_2 physical solubility relies on Lewis acid-base interactions between the acid gas and the absorbent [35–37], being thus more pronounced in solvents with strong electronegative groups. Because of this, the calorific energy requirement to regenerate the solvents in the physical absorption processes is lower than the one from chemical absorption processes.

There have been many physical scrubbing processes developed commercially for acid gas absorption [38], and new candidates for physical solvents are developed each year [39,40]. Many ionic liquids operate essentially as physical solvents [41], and so do the silicone-based hydrophobic physical solvents [42,43] recently presented in literature. In this study, however, we will focus only on commercial solvents. The physical solvents included in our analysis are listed in Table 2. A good review on many of the physical absorption technologies is given by Vega et al. [44], therefore we will only summarize some of the operational peculiarities of these solvents.

- Methanol: Both the Rectisol™ and the Ifpexol™ processes operate with methanol at moderate to high pressures ($p_{CO2} \geq 1$ MPa [45]) and fairly low temperatures, −70 to − 10 °C though the details vary from author to author [38,44–47]. These low temperatures both enhance CO_2 solubility and help avoiding methanol losses due to volatilization.
- N-formyl morpholine: The Morphysorb™ process operates with mixtures of N-formyl-morpholine and N-acetyl-morpholine. Absorption is also carried at moderate pressures, such as $P_{CO_2} \approx 0.8$ MPa in the Kwoen power plant [48] and temperatures between −20 to 40 °C [44]. It is important to remark that NFM has a relatively high freezing point of approximately 23 °C, and thus the addition of N-acetyl-morpholine to the Morphysorb™ solvent comes as a solution for enabling operation at lower temperatures [49].
- N-methyl-2-pyrrolidone: The Purisol™ process uses chilled N-methyl-2-pyrrolidone at temperatures as low as −15 °C [44,47,49], with solvent volatility becoming possibly an issue in case refrigeration is not employed [47,49–51]. Once again, higher CO_2 partial pressures are preferred, for example $P_{CO_2} = 2.4$ MPa [15].
- Propylene carbonate: The Fluor™ process operates with propylene carbonate at high pressures (between 3 and 8 MPa total pressure) and ambient temperatures [44], though chilling can also be employed [47]. There seems to be evidence that the propylene carbonate selectivity for methane instead of CO_2 increases with pressure [38], indicating some sort of competitive absorption. This, coupled with the low tolerance of propylene carbonate to H_2S, makes the Fluor™ process more popular for syngas treating and not for natural gas applications [38,47].
- Poly(ethylene glycol) dimethyl ether: The Selexol™ and Genosorb™ processes are popular alternatives for CO_2 separation [45,52]. The solvent is a mixture of polyethylene glycol dimethyl ethers with chain lengths of between 3 and 9 monomers [45,47,52,53] (the details of this mixture potentially make the difference between the Selexol™ and Genosorb™ solvents [53]). The Selexol™ operates between 0 and 5 °C [44,47], with lower temperatures being avoided due to large solvent viscosity issues [47]. Processes are typically operated in a pressure range from 2 to 14 MPa and treat gases of 5 to 60 %v/v of CO_2 content [50,54].
- Tributyl phosphate: Not much is spoken about the Estasolvan™ nowadays, perhaps because of the low solubility of CO_2 in tributyl phosphate [38,50,51,55]. To our knowledge, this process has never been implemented commercially [38].
- Tetramethyl sulfone: Contrarily to the other solvents mentioned in this section, there is no physical scrubbing process employing tetramethyl sulfone (commonly called *sulfolane*) as a solvent in itself. Instead, sulfolane is mixed with an amine such as diisopropanolamine or N-methyldiethanolamine to form the Sulfinol-M™ solvent. The Sulfinol™ is often called a hybrid process, and has arguably more similarities to chemical scrubbing than to physical scrubbing [38,56–58].

Table 2
Physical solvents for CO_2 absorption and their processes.

Abbreviation	Name of chemical	Process it appears in
Methanol	Methanol	Rectisol™ / Ifpexol™
NFM	N-formyl-morpholine	Morphysorb™
NMP	N-methyl-2-pyrrolidone	Purisol™
PC	Propylene carbonate	Fluor™
PEGDME	Poly(ethylene glycol) dimethyl ether	Selexol™/Genosorb™
TBP	Tributyl phosphate	Estasolvan™
TMS	Tetramethylene sulfone	Sulfinol™

In terms of solvent stability, most organic solvents are apparently resistant to degradation. Evaluation of the Morphysorb™ process in the Kwoen plant shows that N-formyl-morpholine suffers little degradation, being safe to operate at temperatures below 80 °C [48]. The Selexol™ solvent is stable, nontoxic and biodegradable [38,45]. Propylene carbonate is apparently less stable, so that operations should be kept below 65 °C [47] and mixing with water should be avoided [49].

The physical solubility of CO_2 and methane in these organic solvents can be estimated with Henry's law, Eq. (1), where P_i is the partial pressure of the gas and x_i is the equilibrium molar fraction of the gas in the solvent. Eq. (2) shows a temperature-dependent expression for calculating the Henry's coefficient H_i, wherein H_i has the unit of MPa and T has the unit of K. The Henry's relation and the correlation used to estimate the solubility of the gas i is given by:

$$H_i = \frac{P_i}{x_i} \tag{1}$$

$$ln(H_i) = A + \frac{B}{T} \tag{2}$$

Table 3 shows the A and B parameters for different gases in a series of solvents. These parameters have been regressed from different sources in literature, all of which are referred to in Table 3. For regressing the parameters of Eq. (2), we have refrained from using any set of data above 100 °C or in which the molar fraction of gas in the solvent was above $x_i = 0.30$. These measures were taken to reinforce that the resulting parameters are fitted precisely for our region of applicability

Table 3
Henry's law parameters for gas absorption in physical solvents.

Gas	Solvent	A	B	Trange	Sources
CO_2	Methanol	8.328	−1709.8	[−60, 90 °C]	[59,60,61]
	NFM	7.710	−1716.2	[25, 100 °C]	[62,63]
	NMP	7.567	−1682.8	[−20, 100 °C	[64,65,66,67]
	PC	7.858	−1730.5	[25, 100 °C]	[63,64]
	PEGDME	6.032	−1411.3	[25, 70 °C]	[63,53]
	TBP	4.493	−1024.5	[0, 40 °C]	[68,69]
	TMS	7.123	−1471.5	[30, 100 °C]	[64,70]
CH_4	Methanol	5.086	123.26	[−60, 40 °C]	[71,72,73]
	NFM	4.786	101.00	[25, 100 °C]	[62,74]
	NMP	4.926	−166.02	[−20, 25 °C]	[67,74]
	PC	4.808	76.269	[−29, 100 °C]	[75]
	PEGDME	3.137	111.68	[25, 60 °C]	[76]
	TMS	5.086	123.26	[25, 100 °C]	[70]

(between 20 °C and 80 °C, with lower temperatures if possible), and also to make sure that the solubility data does not extend beyond the span of validity of Henry's law approach. It is also true that high temperature solubility data tends to be less reproducible than data at lower temperatures, as can be observed in Fig. 2, this being another reason for avoiding using high temperature data for parameter fitting.

We have not included in our fitting sets of data that differed too much from their counterparts, or that expressed an abnormally high CO_2 solubility. This applies to Rajasingam et al. [77] for NMP and to Chen et al. [78] for TPB. It is difficult to find (and thus evaluate) experimental data for CO_2 solubilities in tributyl phosphate, but the results obtained by Chen et al. [78] seem inconsistent with those obtained by Li et al. [68] and by Thompson et al. [69], and molecular simulation estimates give credibility to the observations of the latter two research groups [79].

The experimental Henry's coefficients of all physical solvents are shown in Fig. 2, together with the curves obtained with Eq. (2) and the parameters presented on Table 3. In molar basis, methanol has the lowest CO_2 solubility and TBP has the highest, and the remainder solvents follow roughly an order of TMS < PC < NFM < NMP < PEGDME.

Though interesting, the series of solubilities seen on Fig. 2 may misrepresent the physical solvents for practical purposes. The fact is that all these absorbents have very different molar masses. Once this is taken into consideration, one ends up with a series of solubilities as seen on Fig. 3 which was plotted by fixing the CO_2 partial pressure at $P_{CO_2} = 100$ kPa and using Eq. (1) with the fitted parameters in Table 3. Now the order of solubilities is almost inverted, with the series following TMS < PEGDME < TBP < NFM < PC < NMP < methanol. This is consistent with mentions in literature regarding the low solubility of CO_2 in TBP [38,50,51,55], and with the appraisal that PC and NMP receive regarding their capacity for CO_2 capture [38,50] (notice that, though TBP seems to have a high capacity for CO_2 capture particularly at high temperatures in Fig. 3, the curve for TBP was extrapolated with data obtained between 0 and 40 °C and might not be representative of real CO_2 solubilities.)

In terms of selectivity for CO_2 in detriment of methane, the solvents perform as shown on Fig. 4. Unfortunately, we were unable to find published data regarding methane solubility in TBP. Nevertheless, Bucklin and Schendel [50] report the selectivity of some physical solvents for CO_2, and among them TBP. As shown on Fig. 4, if the Henry's coefficient data from Table 3 for CO_2 and methane is taken into account, the selectivity for CO_2 follows the order PEGDME < methanol < NMP < PC < TBP < NFM < TMS, though there are discrepancies between the data reported by Bucklin and Schendel [50] and the curves obtained through modelling (also notice that, while Kohl and Nielsen [38] mention the low selectivity of propylene carbonate, this is not observed by Bucklin and Schendel [50]). It is important to remark that the CO_2 selectivity for all solvents increase with a decrease in absorption temperature.

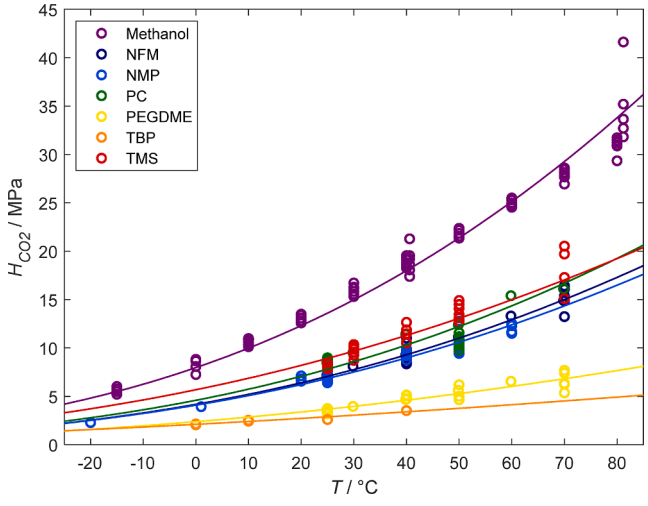

Fig. 2. Experimental Henry's coefficients at different temperatures obtained in literature for a series of organic solvents. The bold lines have been obtained with Eq. (1) and the regressed parameters shown on Table 3.

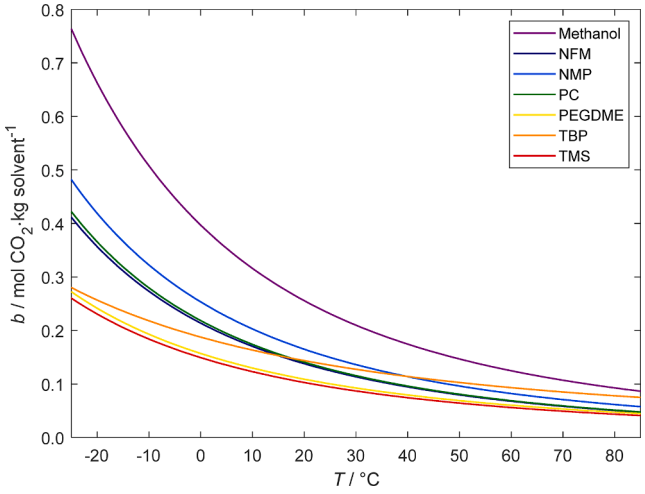

Fig. 3. Molality of CO_2 in equilibrium with 100 kPa of CO_2 partial pressure at different temperatures for a series of physical solvents. The lines have been obtained with Eq. (1) and the regressed parameters shown on Table 3. The molar mass of PEGDME is assumed to be 280 g•mol^{-1} following Bucklin and Schendel [50].

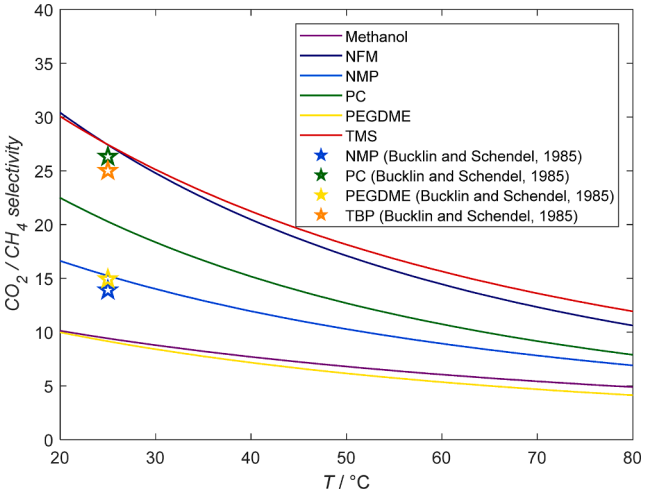

Fig. 4. Selectivity for CO_2 absorption with respect to methane in a series of physical solvents at different temperatures. The lines have been obtained with Eq. (1) and the regressed parameters shown on Table 3. The stars are published data reported by Bucklin and Schendel [50] for 25 °C only.

Physical solvents do not interact strongly with CO_2 during the absorption process, and an evidence of this is the low exothermicity of the chemical phenomenon. The CO_2 heat of absorption may be calculated by application of the van 't Hoff equation (Eq. (3)) to Eqs. (1) and (2), resulting in Eqs. (4) and (5) respectively:

$$\left(\frac{\partial ln(P_i)}{\partial T}\right)_{x_i} = -\frac{\Delta H}{R \bullet T^2} \tag{3}$$

$$\left(\frac{\partial ln P_i}{\partial T}\right)_{x_i} = -\frac{B}{T^2} = -\frac{\Delta H}{R \bullet T^2} \tag{4}$$

$$\Delta H = B \bullet \mathrm{R} \tag{5}$$

The van 't Hoff equation can be used to calculate the heat of absorption ΔH by using the differential of the Napierian logarithm of P_{CO_2} with respect to temperature. Remarkably, one convenience of employing Eq. (2) for the modelling of CO_2 solubilities instead of a more complex expression is that each B-parameter fitted in Table 3 translates linearly into the CO_2 heat of absorption in its respective solvent, as seen on Eq. (5). Note that Eqs. (3)-(5) apply for both CO_2 and CH_4.

The heat of absorption values calculated with Eqs. (4)-(5) and shown on Table 4 are very similar to the ones obtained empirically through calorimetric experiments for physical solvents [80,81]. These calculations were performed with the parameters shown on Table 3 at $T = 20$ °C and $P_{CO_2} = 100$ kPa. Tributyl phosphate has the lowest heat of absorption of all solvents. A low heat of absorption is also observed for PEGDME and TMS. It is an interesting fact that the solvents which show less CO_2 solubility in Fig. 3 also show the lowest exothermicities for CO_2 absorption in Table 4. As for methanol, NFM, NMP and PC, their heat of absorption is essentially the same.

The solubility of CO_2 in water has been obtained by several authors, and the works by Dodds et al. [82] and Diamond and Akinfiev [83] offer good summaries of the published data. For our parametrization of Eq. (5), we have employed four representative datasets covering the temperature span between 0 and 100 °C with special emphasis on low temperature data. Our list of references, as well as the parameters obtained through the regression, can be seen on Table 5. The heat of absorption of CO_2 and CH_4 into water can be calculated with Eq. (5), from which their values are −17.55 kJ/mol and −11.51 kJ/mol respectively.

An important solvent characteristic that should be considered in addition to its absorption capacity and selectivity is the solvent volatility. This solvent property has an important effect on the selection of the operating temperatures. With the sole exception of methanol, all organic solvents evaluated in this study have lower volatility than water (see Fig. 5) (note that some liquid vapor pressures were extrapolated for the sake of completion). In fact, these solvents often have vapor pressures below those of aqueous amines like MEA. Moreover, all physical absorption processes proposed in this investigation are carried out at lower temperatures, and the little amount of solvent that is carried over with the CO_2 product (i.e., due to desorption at higher temperatures) is recovered after pressurization of the CO_2. Hence, the loss of physical absorbent via volatilization is deemed to be negligible in most applications covered in this research. This will be further discussed in section 4.1.1.

Finally, it should be pointed out that our analyses do not consider the impurities in the biogas to be a problem with regards to solvent degradation in the case of physical solvents. As previously mentioned, the main impurities in biogas besides CO_2 are H_2S, NH_3, and then trace amounts of siloxanes, halogenates and VOC compounds [3–6]. Most reports do not mention issues regarding organic physical solvent degradation due to H_2S, with the exception of propylene carbonate [38,47] (in fact, the tolerance of solvents such as PEGDME with regards to H_2S is often mentioned as one of their strengths [47,50]). Siloxanes are harmless to physical absorbents – their main cause of concern is the risk of microcrystalline silica formation, which might be abrasive to equipment downstream of the upgrading plant [92]. Similarly, NH_3 and other contaminants have little to no effect on solvent stability. In summary, degradation in the case of organic physical solvents should not be above what is observed for most solvents. All other issues posed by these secondary contaminants can be easily addressed with a dedicated cleaning station, which is a common feature of most biogas production factories [5].

Table 4
Heat of absorption for a series of physical solvents. Values obtained through Eq. (7). with the parameters presented on Table 3.

Solvent	ΔH/ kJ•mol CO_2^{-1}
Methanol	−14.2
NFM	−14.3
NMP	−14.0
PC	−14.4
PEGDME	−11.7
TBP	−8.5
TMS	−12.2

Table 5
Henry's law parameters for gas absorption in water.

Gas	*A*	*B*	Trange / °C	Sources
CO_2	12.2616	−2110.7	[1,100]	[84,85,86,87]
CH_4	13.0312	−1384.4	[1,71]	[88,89,90,91]

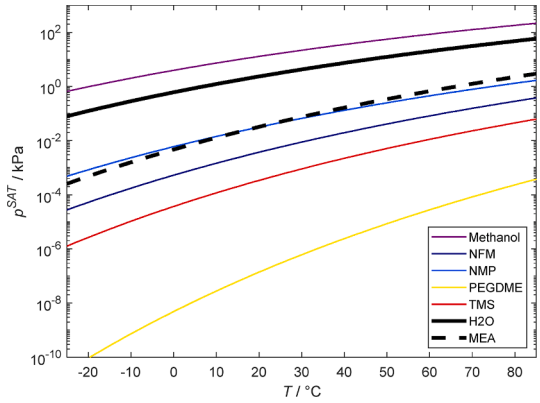

Fig. 5. Saturation pressure (kPa) of different components vs temperature (°C).

2.3. Chemical solvents for CO_2 absorption

The field of CO_2 absorption with amines is vast [25,93] and this section does not intend to carry a full review. Instead, we will focus solely in discussing the nature of the chemical solvent itself.

Solvents for chemical scrubbing of CO_2 are targeted to address a series of practical issues regarding the CO_2 capture process. These issues encompass:

- Capacity and cyclic capacity – Meaning how much CO_2 a solvent in thermodynamical equilibrium can pack between its absorption and desorption cycles. High cyclic capacities mean that less solvent is needed to perform the same amount of CO_2 removal, which implies smaller equipment and perhaps less heating, cooling, and pumping duties.
- Rates – Meaning how fast the CO_2 is absorbed into the solvent. Without fast absorption rates, whatever high cyclic capacities are in equilibrium cannot be achieved in practice.
- Volatility – If one employs volatile solvents, an extra care must be taken to avoid solvent emissive losses. This can result in costly equipment and complex treatment processes [94].
- Viscosity – High viscosities mean all transport phenomena are carried out with more morosity, which affects equipment sizing and energy performances [95].
- Degradation – Thermal and oxidative degradation result in constant reclamation and costly solvent make-up issues. Degradation has an additional impact on corrosion and emissions, being an environmental as well as a financial issue [96].
- Corrosion – Corrosion has been observed to happen in more than half of the typical CO_2 capture plant equipment [97], thus drastically reducing the useful life of the installation.
- Emissions – Emissions might stem from the volatilization of the amine or of its degradation products, presenting a threat to health and environment [98,99]. It must be noted that, in the case of

biomethane production, wherein the treated gas will ultimately be combusted, the issue of emissions can be considered perhaps less of a problem than in cases where the treated gas is released to the atmosphere.
- Toxicity – Solvent toxicity to plant and animal life is clearly an issue of health and environmental concern [100].
- Price – Amines for CO_2 capture should not be too expensive [93].

Previously, the benchmark chemical solvent for CO_2 absorption was aqueous monoethanolamine (MEA). This in itself came out of a technological evolutionary process. In fact, the first amine employed in the chemical scrubbing industry was triethanolamine (TEA) [94]. This amine presented a series of issues (e.g., high viscosity, low absorption rates) and quickly lost ground to MEA, diethanolamine (DEA), N-methyldiethanolamine (MDEA) and diglycolamine (DGA). Of these, MEA presented the largest number of advantages: it has fast mass transfer rates, low viscosity, high capacity, and whatever issues it has that contribute to its losses (e.g., its degradation rates [101], its relatively high volatility) are swiftly compensated by its very low price [93].

The development of amine solvents for CO_2 capture did not end with aqueous MEA. Investigations veered into new aqueous amine solvents containing one single amine [102] and then amine blends [103,104] with great success. Investigations attempted to remove the water off of these mixtures to create water-lean solvents [105], or to shift from alkanolamines to naturally occurring amino acids [106,107]. From single-phase solvents, the solvent has been allowed to form two phases either with liquid–liquid demixing [108] or solid precipitation [109]. This is an extremely long and intricate history of developments that go beyond the scope of this section. What can be said is that aqueous MEA is in a process of losing its relevance as the benchmark amine solvent for CO_2 capture, being substituted either by aqueous piperazine (PZ) [110] or by blends of PZ and 2-amino-2-methyl-1-propanol (AMP) [111]. Meanwhile, it seems that industrial biogas upgrading plants have been using aqueous mixtures of MDEA and PZ more often than aqueous MEA [112–114]. This is supported by Bauer et al. [8,12]. This blend of MDEA with PZ is often called aMDEA (*activated MDEA*) [8,115].

Regardless, most reviews on chemical scrubbing for biogas upgrading still mention aqueous MEA as the benchmark [113,114,116]. For our purposes, we shall join our peers in focusing on aqueous MEA as a representative chemical solvent. This is obviously convenient, as aqueous MEA has been extensively studied and its properties are widely catalogued. Moreover, since we have decided to carry our analysis on the basis of thermodynamic performance while ignoring issues of kinetics and degradation/corrosion (in which one would find vast discrepancies between aMDEA and MEA performances), for us, the main differences between aMDEA and MEA are their distinct vapor–liquid equilibrium behaviors (aMDEA has a slightly higher cyclic capacity [117]) and enthalpies of absorption. With this in mind, results for MEA should not differ excessively from those for aMDEA, as the true advantages and disadvantages of the aMDEA solvent over aqueous MEA are obfuscated from a purely thermodynamic perspective.

In a practical sense, there are two essential thermodynamic quantities that must be well understood for assessing the energy consumption of CO_2 absorption–desorption into a process with aqueous amines. The first one is the solvent capacity and how it shifts with temperature. This is often referred to as the vapor–liquid equilibrium (VLE) of CO_2 in the solvent. The second thermodynamic quantity is the CO_2 heat of absorption, i.e., how much heat is released in the exothermic absorption of CO_2 into the solvent. Even though roughly the same amount of heat must be given to the solvent for its endothermal desorption of CO_2, the energy penalty is still considerably high. Together, these two thermodynamic quantities define both how much CO_2 is released by raising the temperature of the solvent and how much energy has to be spent for releasing CO_2 at high temperatures.

As discussed in the literature [118–120], the use of the van 't Hoff equation in amine systems inherently implies that, among other assumptions, only one reaction is occurring in the system, some species are disregarded and the relation between the molar fractions and the activity coefficients is constant. Even though for physical solvents this approach is reasonable, for amine systems considerable errors have been reported, even if the thermodynamic model is consistent and accurate with respect to the VLE [121,122]. Hence, the empirical method proposed by Kim and Svendsen [118] using differential calorimetry seems to produce more precise results, as it is directly targeted at measuring enthalpy variations in the solvent upon absorption of CO_2.

Some simplified thermodynamic models have been developed and report a constant heat of absorption for the CO_2-MEA-H_2O system [123] of 88.0 kJ/mol. However, for typical reboiler operating temperatures (120 °C), using this averaged value underpredicts the energetic requirements of the reboiler, hence the experimental values reported by Kim and Svendsen are used in this work [118]. By comparing this value to the ones reported by physical solvents (Table 4), it is possible to acknowledge that the chemical solvents will require more calorific energy to carry out the separation, as the CO_2 heat of absorption in those is around 4 to 5 times larger than in physical solvent processes.

A review on the chemical scrubbing process would be superfluous in this stage of our study, as a detailed description of how this process is performed is carried out throughout Section 3.2. For a different approach on process modelling, we invite the reader to consider the works of Moioli et al. [107,124] and Øi et al. [125] employing Aspen Plus and Aspen HYSYS respectively.

3. Process modelling

This section describes the in-house models utilized in the techno-economic assessment of this work. The models were implemented in Matlab 2019b and the thermodynamic properties not referenced in Section 2 were taken from the Aspen Plus v8.6 databank. These parameters are provided in the supplementary information.

Our thermodynamic framework assumes that the vapor phase behaves as an ideal gas, the liquid phase behaves as an ideal mixture and the condensers, reboilers and flash tanks are in thermodynamic equilibrium. Although real gases deviate from the ideal behavior at moderate to high pressures, using the same assumption when comparing the different technologies should not jeopardize the findings of this work.

The main goal of any biogas upgrading plant is to process the feed of a raw biogas stream (F_F) at temperature (T_F), at pressure (P_F) and with a methane composition (z_{CH_4}) in order to produce a biomethane stream (F_B) with a delivery temperature (T_B), pressure (P_B) and methane composition (y_{CH_4}). Furthermore, the processes also deliver a carbon dioxide stream (F_C) at a certain temperature (T_C), pressure (P_C) that mainly contains CO_2 (x_{CO_2}) and usually small quantities of CH_4 (x_{CH_4}).

3.1. Physical and water absorption process

3.1.1. With CO_2 recovery

The flowsheet of the **P**hysical/**W**ater absorption process with **C**O_2 **R**ecovery (PWCR) is shown in Fig. 6. The role of the absorber in the process is to remove the necessary amount of CO_2 from the absorber vapor inlet (F_G) in order to comply with the biomethane composition specification (y_{CH_4}). The CO_2 removal requires the absorber to be operated at a certain pressure (P_A) with a lean liquid solvent stream (F_L) at a given temperature (T_L). The PWCR absorber uses the material balances, equilibrium relations, summation equations and enthalpy balances (MESH equations). Thermodynamic equilibrium is assumed at the bottom of the column (the compressor outlet temperature is adjusted to match the outlet liquid temperature calculated with the energy balance in order to simplify the solution algorithm). The lean liquid solvent stream flow is specified using the liquid to gas ratio (L/G):

$$L/G = \frac{m_L}{m_G} \tag{6}$$

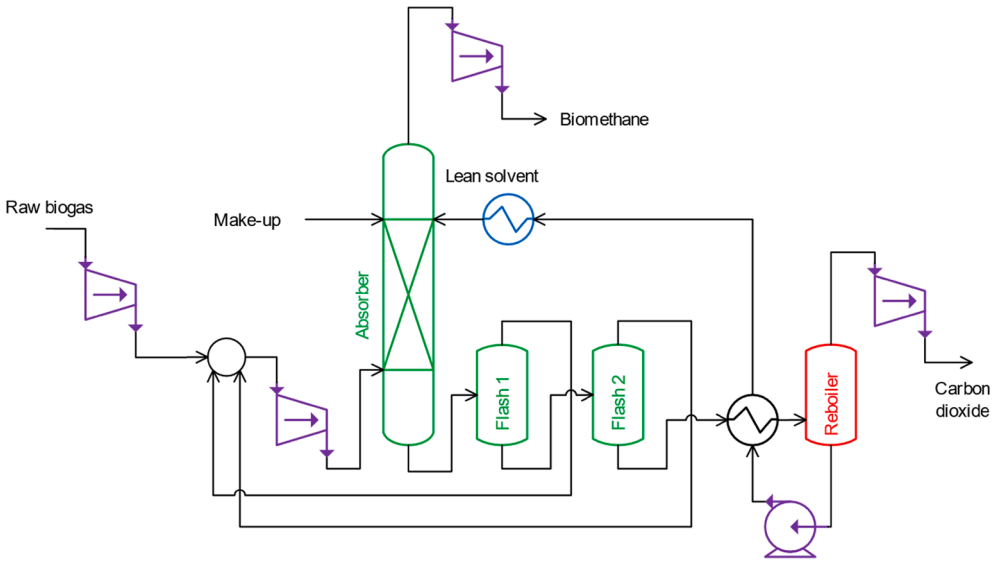

Fig. 6. Proposed process configuration of the physical and water scrubbing technologies with CO_2 recovery (PWCR).

where L/G can be in mass or mole basis. Since both CH_4 and CO_2 are solubilized in the solvent, and the carbon dioxide stream has a specified maximum limit for the amount of methane, part of the methane absorbed must be recovered. This is done by depressurizing the rich solvent stream and then recirculated the vapor that is vaporized from the recycle adiabatic flash tanks. Therefore, only the output pressure of each flash tank can be tuned in order to meet the x_{CH_4} specification. The pressure of the flash tanks must be between the absorber pressure P_A and the reboiler pressure P_R, thus the following relations are proposed:

$$P_1 = (P_A - P_R)\bullet r_P + P_R \tag{7}$$

$$P_2 = (P_1 - P_R)\bullet r_P + P_R \tag{8}$$

where P_1 and P_2 are the outlet pressures of the flash tank 1 and 2 respectively, while r_P is the depressurization ratio (must be between 0 and 1) which represents the fraction of the pressure difference between the inlet pressure and the reboiler. This arrangement is convenient for numerical stability as it ensures that $P_A > P_1 > P_2 > P_R$ while eliminating one degree of freedom. Considering this, r_P can be directly iterated upon in order to comply with the specification in x_{CH_4}.

The heat exchanger shown in Fig. 6 is the result of the heat integration of the biogas upgrading plant and uses a fixed temperature difference in the cold side equal to 10 °C. The computational framework has an implemented algorithm that does not perform the heat integration in cases where heat recovery is not thermodynamically feasible.

The reboiler operation finishes the depressurization cycle by decreasing the pressure from P_2 to P_R and heating the solvent up to a specified reboiler temperature T_R. A temperature increase is usually needed to increase the partial pressure of CH_4 and CO_2 so that the lean solvent has the least amount of solubilized gases. The make-up stream reintroduces the solvent lost due to the evaporation in the reboiler.

Since the carbon dioxide stream is assumed to be fed to a CO_2 transport and storage system, the PWCR requires to comply with a maximum permissible amount of CH_4 in the carbon dioxide stream. Considering this, using a reboiler as the last separation stage instead of a third adiabatic flash tank provides an extra degree of freedom (T_R) that enables the regulation of the carbon dioxide stream compositions. Tuning the compositions without thermal regeneration constraints the operating ranges and, in most cases, it is not possible to find an optimal solution that complies with the specifications of the biomethane and the carbon dioxide streams.

There are four different compressor sections in the PWCR process, each of which has different delivery pressures. The delivery pressure of the feed compressor is the same as the pressure calculated from mixing the vaporized streams from the flash tanks. The absorber compressor section outlet pressure value is identical to P_A. The biogas compressor elevates the pressure from P_A and delivers it at P_B. The CO_2 compressor increases the pressure from the reboiler up to P_C.

One of the main concerns in biogas upgrading technologies is the loss of methane in the process. This is quantified with the methane slip parameter (θ):

$$\theta = 1 - \frac{F_{B,CH_4}}{F_{F,CH_4}} \tag{9}$$

where F_{B,CH_4} is the CH_4 material flow in the biomethane stream and F_{F,CH_4} is the CH_4 material flow in the raw biogas stream.

3.1.2. *Without CO_2 recovery*

The traditional process configuration of physical scrubbing processes regenerates the solvents using air stripping, i.e. stripping the solvent with an air stream that reduces the partial pressures of the CO_2 and CH_4 in the vapor phase and allows the vaporization of the gases by creating a difference in the chemical potential. The **P**hysical/**W**ater process configuration (PW) analyzed in this work has been reported in different sources [126,127] and is presented in Fig. 7. One can notice that, as opposed to the PWCR, the solvent regeneration system of the PW has a heat exchanger and a reboiler instead of a desorber column. The L/G ratio between the rich solvent and the air supply stream in the desorber column is specified and it is used to calculate the composition of the lean solvent exiting the bottom of the absorber.

The vapor stream released from the desorber contains both CH_4 and CO_2. While the amount of CH_4 is expected to be lower than that of CO_2, the greenhouse effect and environmental impact of CH_4 methane is significantly higher when compared to CO_2 [128]. Therefore, the costs associated to the release of CH_4 to the atmosphere are more than 20 times higher than those from releasing CO_2 [129]. In order to eliminate CH_4 emissions, the gas released from the stripper is treated with a regenerative thermal oxidation (RTO) unit that transforms the CH_4 into CO_2. The destruction efficiency of thermal oxidizers can be close 100% [130], hence, in this work, we assume that the CH_4 conversion is 99% and we consider that the RTO operates at 750 °C in order to ensure a complete conversion of methane (the autoignition temperature of CH_4 is 550 °C).

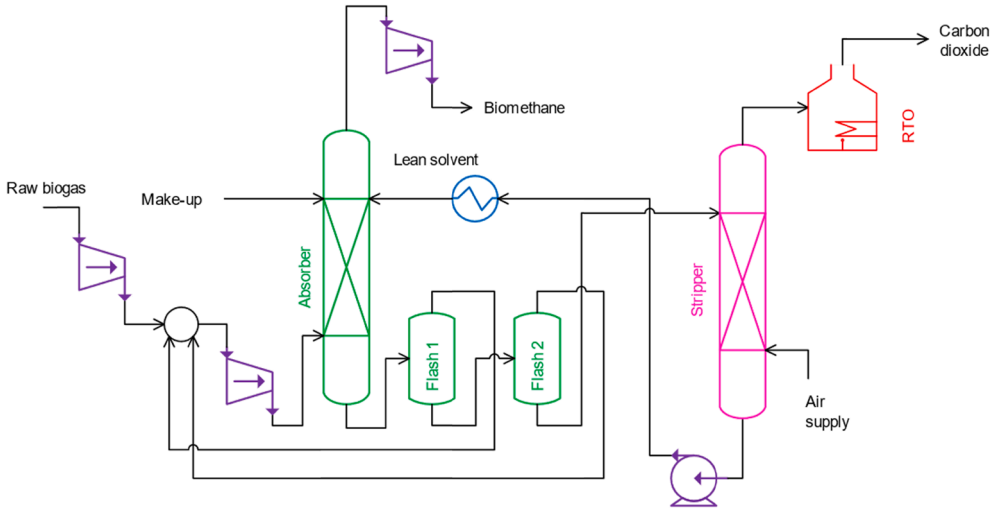

Fig. 7. Proposed process configuration of the physical and water scrubbing technologies without CO_2 recovery (PW).

3.2. Chemical absorption process

The chemical process flowsheet of the **A**queous a**M**ine absorption process without CO_2 Recovery (AM) and the **A**queous a**M**ine absorption process with **C**O_2 **R**ecovery (AMCR) are shown in Fig. 8. As opposed to the physical solvent processes, the process configuration does not change significantly whether CO_2 recovery is considered or not. In fact, the only difference lies on the inclusion of the CO_2 compressor in the carbon dioxide stream.

Considering that in this process most of the CO_2 is solubilized by chemically binding itself to the amine, solvent regeneration is usually carried at low pressures. The vapor–liquid equilibrium behavior is calculated using the machine-learning based surrogate model validated in a previous work [122]. On the other hand, H_2O must be included in the phase equilibria calculations because its partial pressure can be equal or greater than the CO_2 partial pressure. MEA is assumed to be non-volatile because its boiling point is considerably smaller than that of the other components.

The role of the absorber in this process is the same as in the physical absorption processes, but the difference is that the absorber pressure P_A is assumed to be constant and equal to 100 kPa. This process also uses a lean liquid solvent stream (F_L) at a given temperature (T_L), CO_2 loading (α_{Lean}) and a 30 % wt. MEA solvent. Analogously to the physical and water scrubbing process, the (L/G) ratio is used to specify F_L.

The model considers the absorber to be isobaric, adiabatic, and that both phases are in thermal equilibrium at the top. This simplification is justified when one looks at the pilot plant data from Tobiesen et al. [131]. It is reported that, in average, the liquid temperature is 5 °C higher than the vapor phase temperature at the top.

The assumptions done in the absorber allow the estimation of the compositions and the temperature of the outlet streams without using complex differential models like the ones presented elsewhere [131–133]. An inconvenience of this simplification is that it does not estimate the temperature profile, hence the location of a temperature bulge is unknown. A large temperature bulge can lead to an undesired pinch, and the CO_2 mass transfer flux can decrease significantly [134]. Not considering the temperature bulge inevitably underestimates the minimum L/G ratio and the energetic requirement for the separation. In order to consider the temperature bulge effect, a maximum theoretical temperature $(T_{L,Max})$ is calculated by performing an overall mass and

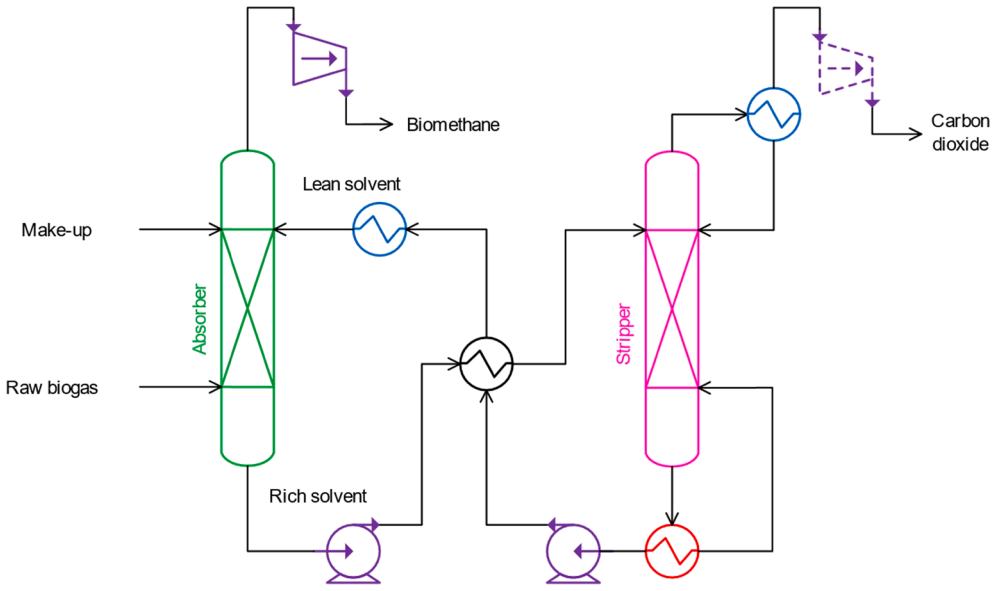

Fig. 8. Process configuration of the chemical scrubbing technology with CO_2 recovery (AMCR) and without CO_2 recovery (AM). The dashed compressor indicates that it is only present in the AMCR process.

energy balance and neglecting water evaporation. Note that the value of $T_{L,Max}$ is always higher than the actual liquid temperature flowing from the bottom of the absorber. In this work we assumed that if $T_{L,Max}$ is estimated to be greater than 90 °C, then the absorber is deemed unfeasible.

The heat exchanger recovers the heat from the reboiler outlet and fixes a temperature difference in the hot side constant and equal to 10 °C. The reboiler temperature (T_R) is specified, and along with α_{Lean} and the aqueous solvent composition, the reboiler pressure can be estimated (P_R). The desorber pressure is assumed to be equal to the reboiler pressure. The temperature difference between the reboiler and the top of the desorber ΔT_D is specified to be equal to 20 °C, while the condenser temperature of the partial condenser of the desorber is 20 °C in accordance to reported plant data [135]. Although a small ΔT_D would require less energy consumption, the size of the desorber would become unfeasibly large.

The carbon dioxide stream (F_C) is produced by condensing most of the water content that exits the top of the desorber. It is important to underline that since the solubility of methane is disregarded in the chemical absorption plant model, x_{CH_4} is equal to 0. The make-up W compensates the amount of water lost in the absorber or desorber.

As opposed to the physical scrubbing processes, the amine-based processes require less compression sections. The AM process only requires the biomethane compressor while the AMCR process requires the compressors for the biomethane and the carbon dioxide streams.

3.3. Auxiliary systems

3.3.1. Compressors

The compressors are modelled as isentropic; hence the following equation can be applied to determine their power consumption [136]:

$$W_K = \frac{m \bullet \left(h_2^* - h_1\right)}{\eta_{K,S} \bullet \eta_{K,M}} \tag{10}$$

where W_K is the compressor power consumption, m is the material flow of the unit operation, h_2^* is the specific enthalpy of the outlet for the isentropic process, h_1 is the specific enthalpy of the inlet, $\eta_{C,S}$ is the isentropic efficiency and $\eta_{C,M}$ is the mechanical efficiency. The efficiency values for the compressors and other auxiliary systems are shown in Table 6.

Since the biogas upgrading processes requires considerable pressure increments, the compression trains must be divided in compression stages. The number of compression stages in each compression section is calculated using the compressor ratio equation [137]:

$$log(CR) = \frac{log\left(\frac{P_a}{P_b}\right)}{n} \tag{11}$$

where P_a is the pressure feed to the compressor sequence, P_b is the outlet pressure of the compressor train, n is the number of compressors and CR is the compression ratio. It is advised that compressors do not work at high temperatures (this work avoids operating compressor temperatures above 150 °C), therefore the maximum value allowed in this work for CR is 4.0 in order to comply with this restriction.

Compression sequences usually include intercooling stages that lower the temperature from the outlet of the compressors to a low intercooling temperature (T_I). This is done to improve the energetic performance of the compressor system and to remove any undesired volatile components from the gas mixture. T_I in this work is fixed and equal to 25 °C for all solvents except for methanol which uses 0 °C because of its high volatility. The intercooling stages in the biomethane and the carbon dioxide streams are used for cooling the compressed gas, removing any organic solvent/water from the gas stream, and recirculating the condensed phase to the make-up stream of the process.

Table 6
Summary of the key variables used in the biogas upgrading processes.

Variable	Process			
	PWCR	PW	AMCR	AM
Process variables				
L/G(absorber)	Independent			
L/G(desorber)	N/A	Independent	Dependent	
$T_L/^\circ C$	Independent			
$T_R/^\circ C$	Independent	N/A	Independent	
P_R/kPa	100	100	Dependent	
r_P	Dependent	Independent	N/A	
α_{Lean}	N/A		Independent	
P_A/kPa	Dependent		100	
Specifications				
z_{CH_4}	0.5 – 0.9			
y_{CH_4}	0.98			
x_{CH_4}	$\leq$ 0.04	Dependent	$\leq$ 0.04	Dependent
T_B/K	298.15			
P_B/kPa	100 – 5,500			
T_C/K	283.15			
P_C/kPa	150,000			
Equipment efficiency				
$\eta_{C,S}/\%$	80			
$\eta_{C,M}/\%$	97			
$\eta_P/\%$	80			
$\eta_B/\%$	70			
Economic variables				
$C_Q/USD \bullet \text{MMBTU}^{-1}$	2.50			
$C_E/USD \bullet \text{kWh}^{-1}$	0.0683			
$C_T/USD \bullet \text{ton}^{-1}$	$\geq$ 0			

* P_R is the desorber pressure in the PW process.

3.3.2. Pumps

Hydraulic pumps are required to compress and transport the liquid solvent. The electrical energy required by a pump (W_P) is given by:

$$W_P = \frac{m \bullet \Delta P}{\rho \bullet \eta_P} \tag{12}$$

where m is the material flow of the fluid, ΔP is the pressure difference between the outlet and the inlet of the pump, ρ is the fluid density and η_P is the mechanical efficiency of the pump. The ΔP is calculated as the pressure difference between the pressure of the connected equipment plus a constant value of 300 kPa in order to account for the pressure drop caused by hydrostatic and frictional forces.

3.3.3. Cooling system

The cooling system is used to cool the service fluid (water) to lower the temperature of the main unit operations in the biogas upgrading plant. This system is composed of a cooling tower, a blower and a hydraulic pump. The equation for estimating the blower power (W_B) is given by:

$$W_B = \frac{m \bullet \Delta P}{\rho \bullet \eta_B} \tag{13}$$

where η_B is the blower efficiency. It is considered that the minimum temperature which can be reached by cooling water with air is $T_U = 20$ °C. The value of T_U is dependent on the geographical location of the biogas upgrading plant. A temperature increase of 10 °C is allowed on the cooling water before it is sent to the cooling tower again. Moreover, a minimum temperature gradient of 5 °C is considered as needed in order to cool a stream, hence, any stream that requires to be cooled less than $T_U + 5$ °C must use a fluid service cooled by the chilling system.

3.3.4. Chilling system

The energy needed by the chilling system is calculated with the coefficient of performance (COP), which is the ratio between the electrical energy consumption of the chilling system (W_F) and the amount of energy that must be removed using the refrigerant (W_{Chill}). The energetic consumption of the chilling system can be calculated by:

$$W_F = COP \bullet \mathrm{W_{Chill}} \tag{14}$$

There has been extensive research in order to improve the energetic efficiency of different chilling systems [138]. The COP of the system is a function of the chilling temperature (T_{Chill}), hence the COP can be calculated with the following empirical equation, which is valid for chilling systems operating with CO_2 as refrigerant and the M−SC configuration as reported by Bellos and Tzivanidis [138].

$$COP = 0.001 \bullet \exp(0.301 \bullet \mathrm{T_{Chill}}) \tag{15}$$

3.3.5. Reboiler

This system provides the necessary calorific energy to heat up the solvent in the reboiler in order to regenerate it. It is considered that the produced biomethane is used as the fuel source. Henceforward, the reboiler duty (Q_R) can be calculated in terms of combusted biomethane (F_{Burnt}):

$$F_{Burnt} = \frac{Q_R}{y_{CH_4} \bullet \Delta H_{CH_4}} \tag{16}$$

where ΔH_{CH_4} is the combustion enthalpy of methane and is equal to 890.5 kJ/mol. In the context of the PW process, the term Q_R is the energy associated to the RTO unit.

3.4. Economic evaluation

The economic assessment of the biogas upgrading technologies of this work captures the effect of the biomethane sold to the user, the operational costs, and the taxes/penalties associated to the release of greenhouse gases to the atmosphere. The concept of integrating the environmental impacts with monetary values has been standardized within the ISO 14008:2019 framework [139]. By considering this, the following equation is proposed:

$$\Pi = \left(0.844 \bullet \mathrm{C_Q} \bullet \mathrm{y_{CH_4}} \bullet (\mathrm{F_B} - \mathrm{F_{Burnt}}) - 0.278 \bullet \mathrm{C_E} \bullet \mathrm{E} - 0.044 \bullet \mathrm{C_T} \bullet \left(\mathrm{x_{CO_2}} \bullet \mathrm{F_C} + 27.8 \bullet \mathrm{x_{CH_4}} \bullet \mathrm{F_C} + \mathrm{F_{Burnt}}\right) - \mathrm{x_S} \bullet \mathrm{F_C} \bullet \mathrm{M_S} \bullet \mathrm{C_S}\right) \bullet \frac{1}{\mathrm{Q_F}} \tag{17}$$

where Π is the unit profit in USD/Nm^3 of processed raw biogas, Q_F is the normal cubic meter of raw biogas, C_Q is the value of the biogas per energy unit in USD/MMBTU, C_E is the electricity price in USD/kWh, E is the total electricity consumption of all the auxiliary equipment in MJ/s, C_T is the CO_2 tax paid in USD/ton CO_2, C_S is the cost of the solvent in USD/ton, the material flows F_B, F_{Burnt} and F_C are in kmol/s and M_S is the molecular weight of the solvent in kg/kmol. The values of C_Q, C_E and C_T are presented in Table 6. The values of C_S were set as follows: 0 USD/ton for water, 600 USD/ton for methanol [140], 2,000 USD/ton for MEA [93], 1000 USD/ton for PEGDME, NMP and NFM (assumed value).

The first term of Eq. (17) is the combined effect of the revenue generated by producing the biomethane minus the cost associated to the reboiler operation, the second term is the cost associated to the electricity consumption of the plant, the third term is the tax or penalty that must be paid for releasing greenhouse gases (CO_2 or CH_4) to the atmosphere, and the last term represents the solvent loses due to solvent vaporization (PW/PWCR) or amine degradation (AM/AMCR). The numeric factor associated to the CH_4 flow implies that the CH_4 emissions are 27.8 times more expensive than those of CO_2. This ratio was estimated by dividing the average emission values reported by Lombardi and Francini [129]. In this equation we assume that the emission taxes ratio remains constant.

In the case that the policies do not require the biogas upgrading plants to pay CO_2 taxes, the last term C_T can be the value of a CO_2 credit. These credits can be sold between different commercial entities. If one wants to use Eq. (17) for the process evaluation with CO_2 credits, then the last constant should be changed from −0.044 to +0.044.

3.5. Key variables summary

The most important variables for each one of the assessed technologies in this work are presented in Table 6. Each variable with an independent tag is an available degree of freedom. The values for the compressor efficiencies were taken from recommended values [141]. The price of biomethane is an average value taken from the energy market [142] and the C_E value is the average retail electricity price for industrial consumers in the U.S. in 2019 [143].

It is important to remark that the integration of CO_2 recovery affects the parameters in which the process can be feasible. If Table 6 is looked at, one can realize that there are 4 degrees of freedom in the 4 processes (x_{CH_4} is considered as a degree of freedom because it is a restriction).

The reboiler/desorber pressures P_R for both the PW and PWCR processes were fixed to be equal to the atmospheric pressure. The reason for this is that operating at lower P_R implies that P_A will be low as well. Operating at low absorber pressure decreases the electricity output of the compressors, thus making the processes economically more competitive.

3.6. Optimization algorithm

Comparing different technologies is a difficult task, especially if the processes greatly differ one from another. Although the PWCR and the PW processes may seem alike at first glance, the fact that the former alternative includes a reboiler entirely changes the process energetic and economic performance. For this reason, in order to have a fair comparison and judgement of each technology, it is suggested to compare the different technologies only when their operating parameters are optimized.

The optimization algorithm in this work aims to identify operating areas in which the different technologies may be economically competitive. Hence, a relaxed optimization method such as the response surface analysis is ideal. This method has been successfully applied to other complex separation methods [144].

The first step involves selecting the specifications of the process and setting the limits of the independent variables. The limits of important variables for the physical and chemical solvents are presented in Table 7.

The minimum and maximum temperature values for the physical solvents were taken from reports of already-existing processes described in section 2. In the case of NFM and NMP, the maximum temperatures were set so that their partial pressure does not exceed 1.0 kPa. The minimum solvent molar composition of water must be kept high in order to avoid hydrate formation [87]. Note that the NFM case assumes that the solvent is a mixture of NFM and N-acetyl-morpholine in order to decrease the freezing point, so that operations at low temperatures are feasible.

The response surface method relies on creating a design of experi-

Table 7
Limits of the operating parameters of the solvents in the optimization.

	PEGDME	NFM	NMP	Methanol	H_2O	MEA
Minimum temperature / °C	0	−20	−15	−60	10	40
Maximum temperature / °C	175	100	60	−10	60	120
Maximum CO_2 molar fraction	0.3	0.3	0.3	0.3	0.03	0.5*

* CO_2 loading: in mol CO_2/mol MEA.

ments (DOE) and then performing the simulations. The process performance is particularly sensitive to the L/G ratio, therefore it was found that it was best to perform the optimization in two steps. First, the simulations were carried at certain conditions (e.g., in the PWCR process, at fixed values of T_L, T_R and x_{CH_4}) and then an univariable optimization method was used to find the best L/G ratio. The full optimization scheme is presented in Fig. 9.

4. Results and discussion

4.1. Physical absorption processes

An overview of the operating conditions and their effect on the energetic and economic performance of both physical scrubbing technologies PWCR and PW is presented in this subsection. The physical solvent PEGDME is used as the case study to exemplify how the techno-economic analysis of the PWCR and PW processes were made. We perform the economic evaluation of four different organic solvents and water.

4.1.1. With CO_2 recovery

An overview of the operating conditions and their effect on the energetic and economic performance of both physical scrubbing technologies PWCR and PW is presented in this section. The physical solvent PEGDME is used as the case study to exemplify how the techno-economic analysis of the PWCR and PW processes was made.

Usually the physical scrubbing technologies are denominated as pressure swing processes because they rely on a pressure difference to perform the separations. This is true for the PW process. However, for the case of PWCR, the inclusion of a reboiler enables a mixed temperature–pressure swing separation. Considering this, the optimal process operating conditions are expected to differ to those from the PW process.

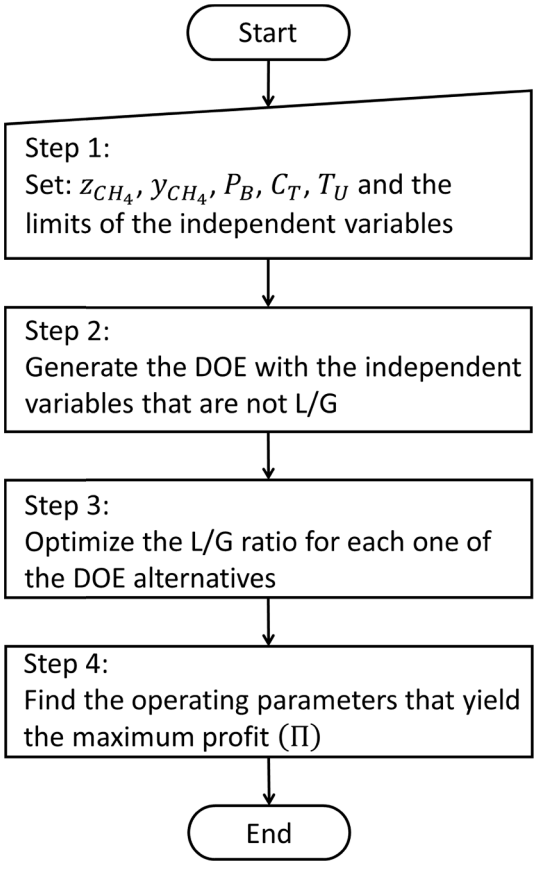

Fig. 9. Optimization algorithm.

An analysis of the PWCR process is presented in Fig. 10 in the form of contour plots. The optimization was done using a 7 level DOE for the T_R and the T_L while $z_{CH4} = 0.7$, $P_B = 1.2MPa$ and $T_U = 20^{\circ}C$. The variables that are not explicitly defined use the values presented in Table 6.

Fig. 10 (a) shows that T_L has a direct relationship with the optimized L/G ratio (kg/kg). This is expected as lower temperatures allow more gas solubilization into the liquid phase, hence less solvent will be required. On the other hand, the reboiler temperature does not seem to have a noticeable effect on the optimized L/G ratio.

The behavior of P_A with respect to the operating temperatures is presented in Fig. 10 (b). It shows that at larger T_L, the absorber operating pressure will be lower. The fact that P_A decreases when T_L is higher may seem counterintuitive, but this behavior is a combined effect caused by the tradeoff that exists between the optimized L/G ratio and T_L: a larger T_L means a larger L/G, which conversely means that the absorber pressure P_A can be lowered.

The effect of T_L on the depressurization ratio is presented in Fig. 10 (c). The recirculation rate of the flash recycle tanks and their corresponding pressure drops are inversely affected by r_P. With a higher T_L, the selectivity CO_2/CH_4 decreases for all physical solvents, and thus the depressurization ratio must be lower to avoid high methane losses.

Fig. 10 (d) presents the calorific energy requirements, where one can observe that the calorific requirement for the PWCR process increases at larger T_L. Although one may expect that larger temperatures would imply lower Q_R, this is not true, because the optimized L/G ratios increase with larger T_L values. This means that the system will spend more calorific energy to heat up the solvent and to desorb CO_2 (note that the calorific energy and all other variables are normalized with respect to the amount of processed raw biogas, hence, Nm^{-3} refers to the normal cubic meters fed to the process).

The electrical energy requirement as a function of the operating temperatures of the process is presented in Fig. 10 (e). The electrical energy consumption is a lumped effect of several energy requirements needed in the process: compression, pumping, cooling system and chilling system duties. Larger T_L values allow the operation of the process at lower pressures (higher L/G), which in turn will reduce the pumping and compression duties. Moreover, the cooling duty is drastically reduced when $T_L \geq 25^{\circ}C$ because the cooling is done with water instead of employing the chilling system. The combination of these effects causes larger T_L to induce less electrical energy requirements.

The combined effect of the calorific and electrical energy can be assessed by observing the profit (Eq. (17)) surface plot in Fig. 10 (f). The effect of T_R on the profit equation indicates that heating the solvent up to 60 to 80 °C has a beneficial effect in the process performance. This is because a larger temperature enables the desorption of more gas from the liquid phase, hence the lean solvent will have less dissolved gases and more capacity to absorb. It is interesting to observe that the surface topology of Fig. 10 (f) is almost symmetrical to that of the electrical energy. This is not a surprise if we consider that, according to Table 6, the cost ratio between the electrical and calorific energy is 8:1. In fact, if the price of electricity is increased significantly, the topology of the electrical requirement and profit response surfaces become symmetrical.

A similar response surface analysis was performed on the PWCR process at different concentrations of CO_2 in the feed and the results are presented in Table 8. It is shown that the optimal L/G ratio has a direct relationship with the value of z_{CH_4}. This behavior is a result of the interaction between the L/G ratio and the molecular weight of the gases. Although the total amount of gas in mass basis is decreasing with larger CO_2 concentrations, the total amount of gas in mole bases is increasing, which means that a larger higher quantity of solvent will be needed to keep a lower pressure.

The analysis on these results also suggest that the dependency of the optimized T_L and T_R with respect to z_{CH_4} is not significative. However, this is not the case for all process variables as r_P, θ and E have a smooth inverse relationship when compared to z_{CH_4}. The results show that at

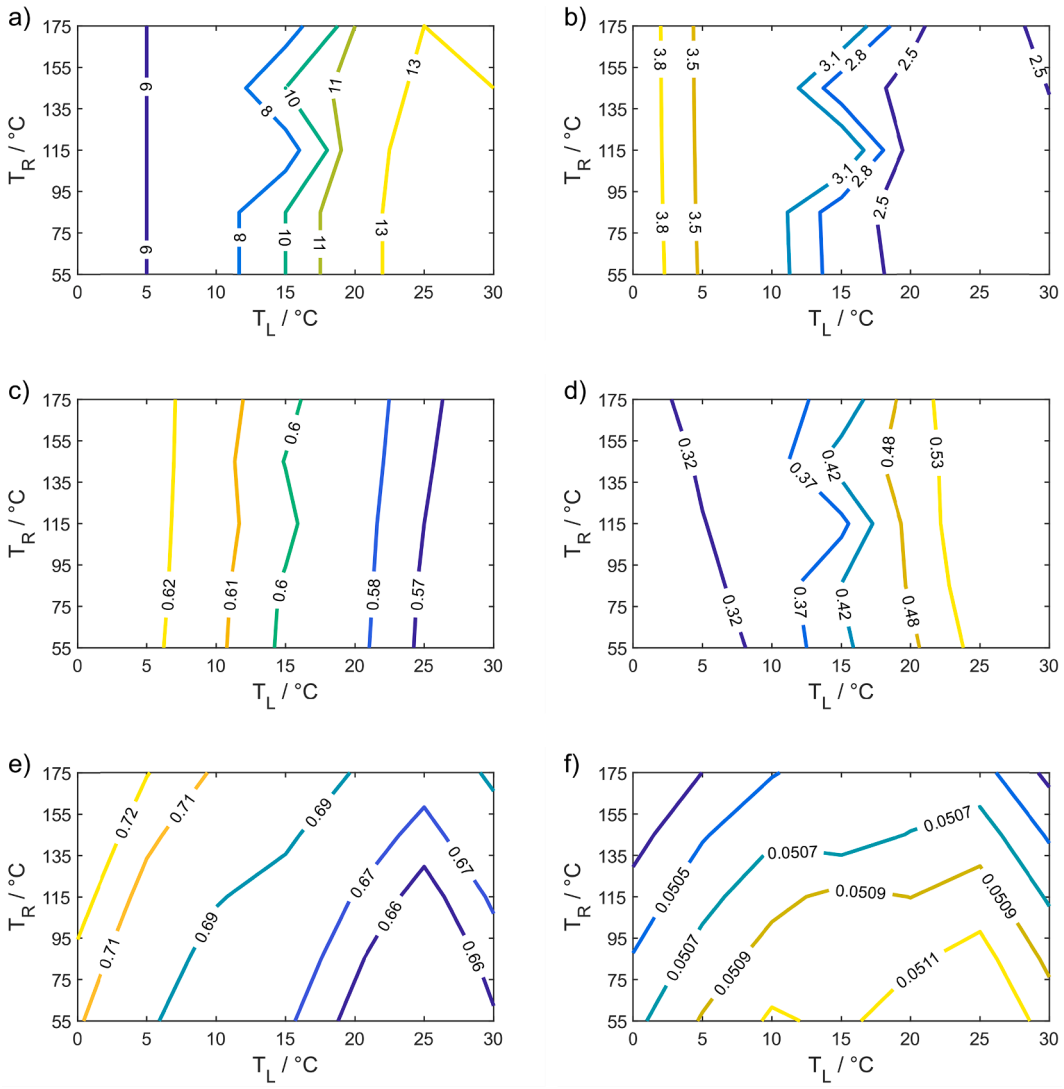

Fig. 10. PWCR process contour plots of: (a) L/G in kg/kg, (b) absorber pressure P_{Abs} in MPa, (c) depressurization ratio r_P, (d) Q_R in MJ/Nm^3, (e) E in MJ/Nm^3 and (f) Profit Π in USD/ Nm^3. $z_{CH4} = 0.7$, $P_{Bio} = 1.2MPa$ and $T_U = 20^{\circ}C$. Solvent: PEGDME.

Table 8
Optimized parameters of the PWCR process using PEGDME as the solvent.

z_{CH_4}	0.5	0.6	0.7	0.8	0.9
L/G (kg/kg)	10.5	12.5	14.5	17	20
T_L/ °C	25	25	25	25	25
T_R/ °C	70	70	70	70	70
P_A/ MPa	2.4	2.3	2.2	2.1	2.1
r_P	0.76	0.67	0.57	0.44	0.27
P_R/ MPa	0.1	0.1	0.1	0.1	0.1
x_{CH_4}	0.04	0.04	0.04	0.04	0.04
θ	0.041	0.027	0.017	0.010	0.004
Lean solvent molar fraction	0.99	0.99	0.99	0.99	0.99
Rich solvent molar fraction	0.67	0.72	0.76	0.80	0.84
Q_R/ MJ/Nm^3	0.59	0.58	0.56	0.54	0.51
E / MJ/Nm^3	0.77	0.70	0.64	0.60	0.57
P_B/ MPa	1.2	1.2	1.2	1.2	1.2
K_C/ %	59.4	52.5	43.6	31.8	18.2
Profit Π / USD/Nm^3	0.029	0.040	0.051	0.062	0.072

larger z_{CH_4} the depressurization ratio must be lower, hence the recirculation of the recycle tanks must increase as well. The cause of this is that larger z_{CH_4} involves more CH_4 dissolved in the mixture, which must be removed from the solvent so that the carbon dioxide stream can meet the specification of x_{CH_4}. The reduction in the methane loss and the operating costs eventually cause that the profit increase proportionately with respect to z_{CH_4}. This is reasonable as it is easier to perform a separation from $z_{CH_4} = 0.9$ to $z_{CH_4} = 0.98$ than if the separation starts at $z_{CH_4} = 0.5$.

The share of the costs associated to the conditioning of the carbon dioxide stream (K_C) is shown in Table 8. These costs include the electricity consumed by the compressors and the cooling power needed in their interstage cooling sections. The inverse relationship between K_C and z_{CH_4} is caused by the reduction of the material flow in the carbon dioxide stream with a larger CH_4 feed concentration.

A comparison of five different physical solvents (4 organic solvents and water) is presented in Fig. 11. The organic solvents PEGDME, NFM and NMP seem to be equally competitive over almost all compositions of z_{CH_4}. Due to the high methanol volatility, the process must be operated at cryogenic temperatures. This causes considerable electricity demands due to the additional dependence on the chilling system. However, this is not the only cause of economic loses, the methanol that cannot be recovered within the compression system should also be replaced. While more than 99.99% of the evaporated PEGDME, NFM and NMP can be recovered in the interstage cooling systems, only 98–99% of the methanol can be recovered. Although the methanol loss may seem low one

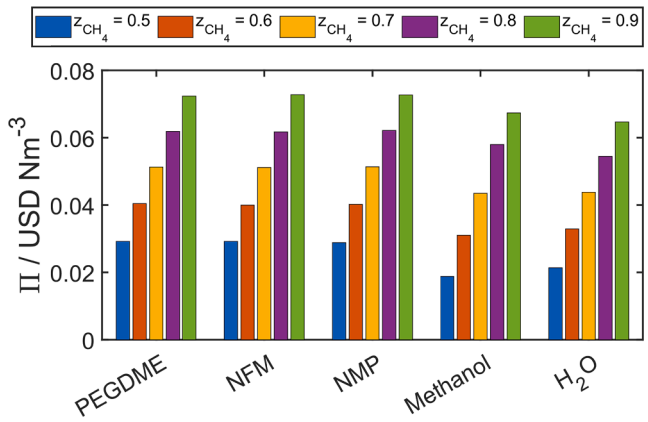

Fig. 11. Profit Π of each one of the solvents using the PWCR process technology at different methane concentrations in the feed.

should consider that adding an extra component into the CO_2 transport and storage systems may raise unforeseen operating issues. Despite the fact that the water absorption capabilities are worse than those of methanol, its low volatility and negligible prices make it more economically competitive at lower z_{CH_4}. Nonetheless, neither methanol nor water seem to be economically competitive.

It is interesting that, despite the fact that PEGDME, NFM and NMP have different thermodynamic properties, they seem to be equally competitive. For example, PEGDME has the worst selectivity of all the compared solvents, however, this is compensated with having the lowest Henry's coefficient (3.7 MPa at 25 °C) and a high boiling point (>250 °C). This last property implies that the solvent can be regenerated at higher temperatures without incurring into considerable solvent losses. On the other hand, NFM and NMP have higher Henry's coefficients (e.g. 7.1 and 6.8 MPa at 25 °C respectively) than PEGDME, but their higher selectivity and lower molecular weight outweigh the lower CO_2 solubility. The lower Henry's coefficient of PEGDME may be advantageous from a capital costs perspective as it means that the shell thickness of the absorber will be smaller and, therefore, more economical.

The PWCR processes operate at relatively low temperatures (less than 100 °C) and medium to high pressures (up to 50 bar), hence a moderate equipment thickness is expected. It is recommended to use carbon steel in physical solvent processes because the organic solvents are noncorrosive. However, this is only valid if the process is not operated at cryogenic temperatures [145]. Unfortunately, this is the case for the methanol and NFM processes which require stainless steel 304L that can be around 2.4 times more expensive than regular carbon steel [130]. The high capital costs associated to the use of stainless steel together with its average economic performance renders the methanol and NFM processes in a less competitive spot when compared to PEGDME and NMP.

Water seems to not be energetically or economically competitive in the PWCR because its Henry's coefficient is around 10 to 20 times greater than in the studied organic solvents. This indicates that the process will be required to operate at larger pressures, and hence, the electricity consumption will be larger. Moreover, larger L/G ratios are needed in order to counter the large Henry's coefficient values and to avoid hydrate formation. This causes that its economic performance is around 10 to 25% worse than the competing technologies. In addition to this, since the solubilization of CO_2 into water produces an acidic mixture, it is necessary to use stainless steel to avoid corrosion and the capital costs of the equipment will increase by a factor of 2.4–3.4 (depending on whether stainless steel 304L or 316L is used) [130].

Due to the similar competitiveness of the PEGDME and NMP, it is important to consider the transport properties. In particular, viscosity is an important property as it may increase significantly the equipment size if it is too large. In Table 9 we include the minimum and maximum viscosity values that can be found in the PWCR process. From this perspective, the solvent competitiveness could be rearranged as H_2O > NMP > Methanol > PEGDME > NFM (the actual viscosity values of the NFM-based solvents also accounts for N-acetyl-morpholine). Although NFM, methanol and H_2O have competitive viscosities when compared to the other organic solvents, their thermodynamic and corrosion-related disadvantages are too substantial to be countered by low viscosities alone.

Providing a definite conclusion about whether PEGDME or NMP is better might not be possible without performing a detailed engineering design. However, an analysis on the optimal T_L for each solvent, might suggest that PEGDME has a slight advantage because the T_L in all cases is 25 °C while the minimum temperature of NMP is 15 °C. This implies that PEGDME, might not require chilling equipment. Nonetheless, we remark, the decision of the optimal solvent requires a thorough analysis that considers the plant location, solvent availability, solvent price and capital investment requirements.

4.1.2. *Without CO_2 recovery*

It is not possible to fully understand the difference between the processes with CO_2 recovery and without CO_2 recovery by only analyzing the effect the of compression system. For this reason, the same optimization procedure was performed on the PW process at different z_{CH_4} conditions when using PEGDME as the solvent. The results of these calculations are shown in Table 10.

The L/G ratios in the PW process are highly influenced by z_{CH_4}. In contrast to the PWCR process, the L/G ratios in the PW process are significantly larger than in the PWCR process. This suggests that the PWCR process relies more on the pressure increase to perform the separation while the PW process depends more on the solvent flow. Since the PWCR process requires higher absorber pressure, the pressure drop between the absorber and the recycle tanks is enough to be able to vaporize the methane and reduce its concentration in the desorber vapor outlet. Nonetheless, it is more expensive to operate the process at larger pressures, therefore, the optimal L/G values in the PW process tend to be higher than in the PWCR process.

Another significant difference is the optimal T_L. While for the PWCR process larger temperatures are preferred, for the PW it seems to be the opposite. This can be explained by considering the fact that a low T_L reduces the absorber pressure and that the PWCR has to operate at larger pressures in order to comply with the x_{CH_4} restriction.

Although the PWCR process relies on a chemical potential shift caused by a combined temperature and pressure swing in contrast to the PW process, the PWCR requires less input calorific energy. This is caused by the implementation of the RTO. We can observe in Table 10 that the amount of calorific energy used to abate the methane in the PW process is significantly higher than in the reboiler of the PWCR process. This is because the PW process increases the temperature from low temperatures to around 750 °C, while the PWCR process increases the temperature of a liquid around 50–70 °C. Moreover, the share of the costs associated to the carbon dioxide stream conditioning – K (i.e., the operating costs of the RTO system) is significantly higher at low z_{CH_4}.

Table 9
Solvent viscosity as a function of the operating temperatures.

Solvent	Viscosity / mPa•s at lowestT_L	Viscosity /mPa•s at highestT_R	Source
PEGDME	6.5 at 25 °C	2.4 at 70 °C	[146]
NFM*	17.1 at − 20 °C	8.3 at 25 °C	Aspen Plus v8.6
NMP	1.5 at 15 °C	1.1 at 54 °C	[147]
Methanol	3.25 at − 60 °C	0.8 at 0 °C	[148]
H_2O	1.31 at 10 °C	0.5 at 47 °C	[149]

* These values account for the mixture between N-formyl-morpholine and N-acetyl-morpholine.

Table 10
Optimized parameters of the PW process using PEGDME as the solvent when $C_T = 0$.

z_{CH_4}	0.5	0.6	0.7	0.8	0.9
Absorber mass basis L/G	143	123	107	82	42
Desorber mass basis L/G	300	300	300	300	300
T_L/ °C	0	0	0	0	0
r_P	0.05	0.05	0.05	0.05	0.05
P_R/kPa	100	100	100	100	100
$x^*_{CH_4}/\ 10^6$	161	183	239	299	284
θ	0.02	0.02	0.01	0.01	0.00
Lean solvent molar fraction	0.98	0.98	0.98	0.98	0.98
Rich solvent molar fraction	0.95	0.95	0.94	0.94	0.91
Q_R/ MJ/Nm^3	1.38	1.08	0.76	0.47	0.21
E / MJ/Nm^3	0.23	0.27	0.29	0.33	0.38
P_B/ MPa	1.2	1.2	1.2	1.2	1.2
K / %	40.2	31.5	22.6	13.7	5.7
Profit Π / USD/Nm^3	0.039	0.048	0.058	0.067	0.077
Profit with integrated heat Π / USD/ Nm^3	0.042	0.051	0.060	0.069	0.077

* In an air-free basis.

This can be explained by analyzing the absorber L/G, the smaller the L/G rate is, the less amount of liquid will be fed to the desorber and, hence, less air supply flow rate will be needed to be heated. Note that the carbon dioxide stream in the PW process is a mixture of CH_4, CO_2, air and evaporated solvent. This additional complexity of the PWCR process gives an economic disadvantage with respect to the PW process. More than 95% of the calorific energy penalty can be removed if a cross heat exchanger is used to recover the energy of the carbon dioxide stream. If a heat exchanger is added, the profit increases between 1% for larger z_{CH_4} and 5% for smaller z_{CH_4}.

Comparing both processes when there is no penalty for the CO_2 emissions is intrinsically unfair, as the PWCR process was developed to comply with the specifications of both biomethane and carbon dioxide streams.

The economic performance of the PW process as a function of C_T is presented in Fig. 12 using PEGDME as a study case. Fig. 12 highlights that processes with less z_{CH_4} will be more affected if the biogas upgrading process has not implemented CO_2 recovery. Furthermore, Fig. 12 also shows the break points in each one of the methane concentrations isolines. A break point is the value of the CO_2 tax in which the PWCR process and the PW processes have the same economic competitiveness. From the break point onwards, the PWCR process will always be economically more competitive. It is important to underline that since the processes with CO_2 recovery do not have CO_2 emissions, their optimal operating conditions are independent of the C_T value. In most cases, the value of the CO_2 tax in the break point is around $12 USD/ton$.

The values of the CO_2 tax depend on the geographical area in which the biogas upgrading plant is to be built. Therefore, analyzing the breakpoint may be important to forecast the upgrading plant revenues, and most importantly, to decide whether the implementation of CO_2 recovery into the process is feasible or not.

These results assume that the biomethane plant must pay CO_2 taxes. If the biomethane plant sells CO_2 credits, then the results would be linearly translated to higher profit values (this can be seen in the fact that Eq. (17) has a linear dependence on C_T).

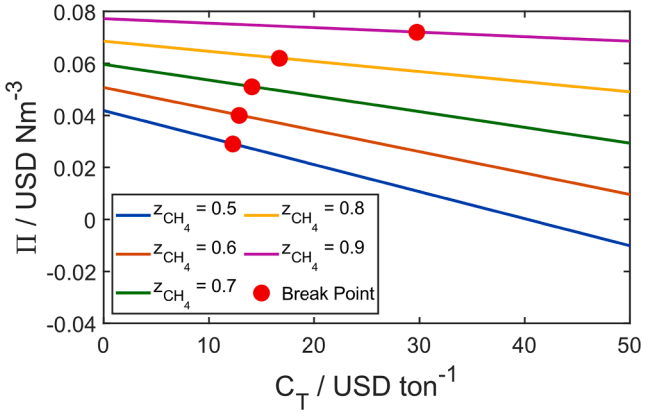

Fig. 12. Dependence of the PW process profit Π as a function of the CO_2 tax value. The break point is the CO_2 tax value in which the PW and PWCR have the same economic performance. Solvent: PEGDME.

4.2. Chemical absorption processes

In the case of chemical scrubbing, the difference between the AMCR and AM processes is minimal because the only discrepancy is the carbon dioxide stream compressor. For this reason, the AMCR and AM processes share the same optimal operating conditions.

In the same fashion as the physical scrubbing processes, the operating parameters were optimized following the algorithm of Fig. 9 and considering the constraints given in Table 7. The results of the optimization algorithm are presented in Table 11.

The main advantage of the chemical absorption processes over the physical absorption processes is the high selectivity of CO_2 and negligible loses of methane, hence, the production of biomethane is maximized with chemical scrubbing. The results show that larger z_{CH_4} require lower solvent flow rates because a smaller amount of CO_2 needs to be captured. Furthermore, a low concentration of CO_2 in the lean solvent requires less calorific and electric energy because smaller liquid solvent flow rates imply lower calorific and electric energy requirements. However, low CO_2 loading values (less than 0.2) are not desirable, because at lower loadings the energy required to perform the regeneration increases considerably.

Assuming that the effect of methane on the AM process is similar to nitrogen, the last case in Table 11 can be compared to the removal of CO_2 from the flue gas of a coal plant using MEA as a solvent. The value of $Q_R = 0.69 MJ/Nm^3$ when $z_{CH_4} = 0.9$ is equivalent to 3.64 GJ/ton of CO_2 captured, which is similar to what is usually reported for the conventional setup of CO_2 capture with aqueous MEA at 30 %wt. [135]. Contrarywise, for $z_{CH_4} = 0.5$, estimated reboiler duties are reduced to 1.62 GJ/ton of CO_2 captured. Although the amount of heat needed is less than in the case with high methane concentration, the economic performance is inferior. This is because higher CH_4 concentration implies more biomethane sold and lower CO_2 tax/credits.

One of the main operating concerns in amine-based chemical scrubbing plants is the thermal and oxidative degradation of the solvent.

Table 11
Optimized parameters of the AM and AMCR processes using 30 %wt. MEA as the solvent.

z_{CH_4}	0.5	0.6	0.7	0.8	0.9
Absorber mass basis L/G	13.5	12	10	7	4.5
α_{Lean}	0.24	0.24	0.24	0.24	0.30
T_L/ °C	40	40	40	40	40
T_R/ °C	120	120	120	120	120
α_{Rich}	0.50	0.50	0.50	0.50	0.50
Q_R/ MJ/Nm^3	4.13	3.28	2.42	1.55	0.69
E– AM / MJ/Nm^3	0.28	0.31	0.35	0.38	0.42
E– AMCR / MJ/Nm^3	0.97	0.86	0.75	0.64	0.54
Profit Π (no degradation) / USD/ Nm^3	0.019	0.032	0.046	0.059	0.073
Profit Π (maximum degradation) / USD/Nm^3	0.012	0.027	0.041	0.056	0.071

Chemical absorption plants using MEA to remove the CO_2 from a coal-fired plant have reported amine degradation values between 0.3 kg and 3.6 kg/ton CO_2 [150]. Due to the lack of oxygen in the biogas upgrading feed, we expect a lower degradation rate, hence, the degradation boundaries are set to be between 0 and 3 kg/ton CO_2. Table 11 shows that the economic impact of amine degradation decreases with larger z_{CH_4} due to a lower requirement of amine solvent. This effect is quite pronounced at low z_{CH_4}, where degradation can reduce the profit up to 35% at maximum degradation conditions.

The difference between the AMCR and AM processes in the electrical energy consumption is the carbon dioxide compressor. In the case of the AM process, the electricity demand increases slightly when z_{CH_4} increases because the amount of gas that needs to be compressed increases as well. Conversely, the electrical demand decreases when the amount of methane increases because the delivery pressure specification of the biogas $P_B = 1.2MPa$ is significantly lower than the delivery pressure of the carbon dioxide stream $P_C = 15MPa$.

The breakpoint plot of the AMCR and the AM process is presented in Fig. 13. One can realize that z_{CH_4} does not have a significant influence in the location of the breakpoints, which means that most of them are located when the CO_2 tax is around $10USD/ton$. Furthermore, the breakpoints are located at lower C_T values, which indicates that the extra costs related to the compression of the carbon dioxide stream are low compared to the tax that must be paid for CO_2 emissions.

The capital costs of the AM process will increase with larger amounts of methane in the biogas, because the biomethane compressor must become larger, and thus, the investment costs become larger as well. However, this is not the case for the AMCR process, where capital costs associated to the compressors will be reduced when z_{CH_4} is increased. This is caused by the fact that $P_B < P_C$, hence, the less amount of gas that is needed to be pressurized to 150 bar, the smaller the compressors will be (the same effect is found in the PWCR process). The AMCR process operation will always be more expensive than the AM process because of the extra compression system.

The size of the absorber will not change significantly at different z_{CH_4} because its diameter is mainly a function of the gas surface velocity [151] and the total amount of biogas entering the absorber is always the same. Conversely, the larger the amount of CO_2 in the feed (low z_{CH_4}), the more gas the desorber must process and, hence, it will be larger and more expensive.

Since the amine-based processes are operated at mild temperatures and pressures, the equipment thickness is expected to be minimum when compared to the PWCR process. Unfortunately, due to the corrosive nature of aqueous amine mixtures, it is required to use stainless steel 304L or 316L (the latter is recommended in order to avoid failures [152]). Stainless steel 316L can be 3.4 times more expensive [130] and will increase significantly the capital costs of the plant.

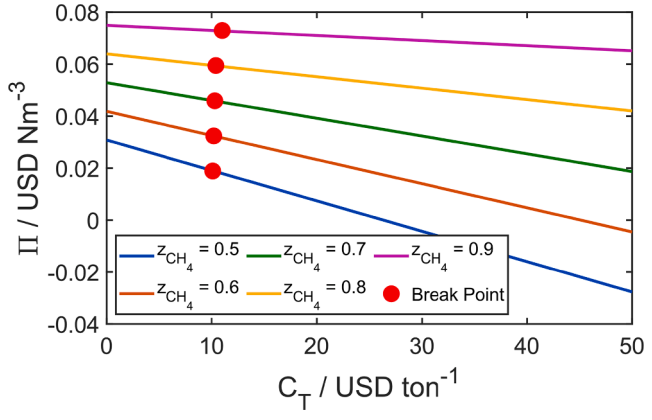

Fig. 13. Dependence of the AMCR process profit Π as a function of the CO_2 tax value. The break point is the CO_2 tax value in which the AM and AMCR have the same economic performance. Solvent: 30 %wt. MEA with no degradation.

4.3. Selection of the optimal technology

In the previous sections, it was shown that, at moderate CO_2 tax values, the PWCR and the AMCR processes seem to be economically more feasible that their counterparts without CO_2 recovery. For this reason, and because of environmental interests, this subsection will focus only on the processes that involve the CO_2 recovery.

If the profit values reported for the PWCR and the AMCR are compared, one can notice that the PWCR process is more profitable than the AMCR process when z_{CH_4} is between 0.5 and 0.8. Conversely, the chemical scrubbing process has better performance at higher methane compositions. One of the main reasons on why the PWCR process has better performance than the AMCR process is because it uses a combined pressure and temperature swing to perform the separation. Contrarywise, the AMCR process relies only on a temperature swing, hence, the energy used to regenerate the solvent can be said to be lost because it does not give any added value to the final product (the biomethane stream at P_B). In contrast, the electrical energy spent in the PWCR process to increase the pressure not only serves to separate the raw biogas mixture but also gives an added value to the final product.

The profit of each one of the processes should change as a function of P_B (as shown in Fig. 14). One can observe that the AMCR process profit increases at higher z_{CH_4} while it decreases at higher P_B. The reason for this effect is because $P_B < P_C$, which indicates that the larger the CO_2 concentration, the higher the electric consumption. The profit decreases with larger pressures because more electrical power is required to compress the biomethane stream. On the other hand, for the PWCR process, the profit (Π) seems to not be affected by P_B. This is because the absorber pressure P_A is larger than the delivery pressure of biomethane P_B, therefore, the last compressor is deemed unnecessary and, therefore, less capital cost investments are required.

If the PWCR and AMCR processes are compared, it is possible to notice that when P_B is equal to 0.1 MPa, there is a crossover in the profit lines, which means that when P_B is low, then it is preferable to use an AMCR process at larger feed methane compositions ($z_{CH_4} > 0.7$) values. Conversely, when the delivery pressure P_B is $1.2MPa$, the AMCR process loses competitivity due to the extra costs caused by the higher compression duties.

In order to provide a guide on which technology to choose based on the methane concentration z_{CH_4} and the delivery pressure P_B, Fig. 15 was generated. A technology is reported as being superior if the difference between the optimized profit between the AMCR and the PWCR process is larger than 5%. Since the degradation values in the AMCR process are somewhat uncertain, an average value of 1.5 kg of degraded MEA/ton CO_2 was used for the calculations in Fig. 15. In the case where the AMCR

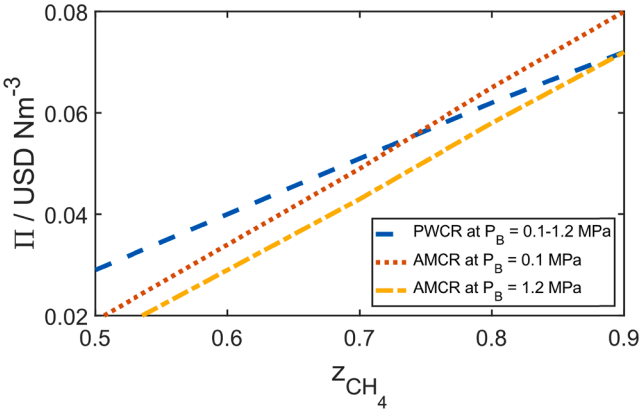

Fig. 14. Effect of P_B and z_{CH_4} on the profit Π of the PWCR and AMCR processes using PEGDME and MEA as solvents.

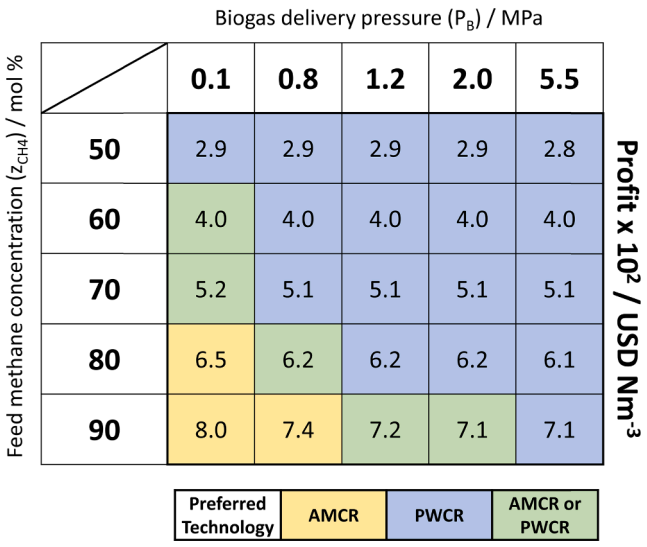

Fig. 15. Technology selection for processes with CO_2 recovery.

and PWCR processes have very similar competitiveness (marked with green in Fig. 15), further evaluations are required to determine the best option. These evaluations should consider that both processes have inherent disadvantages caused by their high operation pressures (PWCR) or corrosive solvents (AMCR) that might reflect on higher capital costs.

Fig. 15 shows that the competitiveness of the PWCR processes increases at higher delivery pressures. This is because the PWCR process uses the pressure increase for two purposes: to perform the separation and to reach the delivery pressure P_{CH_4}. The AMCR process spends the same amount of calorific energy just to regenerate the solvent, while the electric energy always increases when P_B is augmented.

We want to remark that when the study case fixes $z_{CH_4} = 0.9$ and $P_B = 0.1MPa$, the biogas upgrading plant behaves similarly to CO_2 capture processes from flue gases (usually the CO_2 composition is 10–12% mol/mol in coal-fired power plants). At these conditions, the AMCR process seems to have better economic performance. This finding agrees with what has been widely discussed about CO_2 capture processes from flue gases: the amine-based separation processes are expected to outperform processes that require pressurization because of the compression work [24,153]. This is because the CO_2 capture systems have a "clean" stream that flows out from the absorber with a low concentration of CO_2 and a low pressure equal to 1 bar. For this reason, any kind of energy spent to modify the pressure or temperature of the gases that are not CO_2 can be considered to be unnecessary.

5. Conclusions

The energetic and economic assessment of 5 physical solvents was performed. These solvents are PEGDME, NFM, NMP, methanol and water. It was concluded that all of them are capable of upgrading biogas with a CO_2 recovery system, delivering both biomethane and CO_2 within the required specifications. The performance of the solvents can thus be arranged in terms of economic, energetic and expected capital costs in the following order: PEGDME ≈ NMP > NFM > methanol > water.

The feasibility of implementing CO_2 recovery into liquid solvent-based processes was evaluated. It was found that it is necessary to consider the CO_2 tax into the assessment of the biogas upgrading technologies because, at relatively low CO_2 tax values (between 10 and 15 USD/ton CO_2), the processes with CO_2 recovery are economically more competitive than their counterparts without CO_2 recovery.

The optimal technology for biogas upgrading plants is a function of the methane concentration in the feed (z_{CH_4}) and the delivery pressure of the biogas (P_B). Processes using amine solvents are favored at lower z_{CH_4} and lower P_B values, while the physical solvents are favored at larger P_B.

The physical absorption processes outperform the modelled chemical solvent process based on 30 %wt. MEA at moderate to high pressures because the physical absorption uses the compression duty to separate the raw biogas mixture, partly regenerate the solvent, and achieve the delivery pressure specification P_B. In this way, the energetic usage is optimized. On the other hand, the amine processes use the calorific energy to regenerate the solvent, hence all the energy spent on the CO_2 desorption is not used on any other part of the process. It should be remarked that increasing the absorber pressure in case of chemical absorption would lead to different results.

Funding

This research was funded by the Faculty of Natural Sciences of the Norwegian University of Science and Technology (NTNU).

Table of symbols

Symbol	Unit	Meaning
A, B		Henry's coefficient parameters
b	mol/kg solvent	Molality
COP		Coefficient of performance
CR		Compression ratio
C_T	USD/Nm^3	Carbon tax
E	MJ/Nm^3	Electric energy
F	kmol/s	Molar flow rate
H	MPa	Henry's coefficient
h	kJ/kg	Enthalpy
K	%	Share of the costs associated to the carbon dioxide stream conditioning
L/G		Liquid-to-gas ratio
M	kg/kmol	Molecular weight
m	kg/s	Mass flow rate
n		Number of compression stages
P	kPa	Pressure
Q	MJ/Nm^3	Calorific energy
r_P		Depressurization ratio
T	K	Temperature
x		Mol fraction in CO_2 stream
W	kW	Compressor work
y		Mol fraction in biomethane stream
z		Mol fraction in raw biogas stream
Greek symbols		
α	mol CO_2/mol amine	Amine loading
ΔH	kJ/mol CO_2	Heat of absorption
$\eta_{K,S}$		Isentropic efficiency of compressor
$\eta_{K,M}$		Mechanical efficiency of compressor
η_P		Mechanical efficiency of pump
θ		Methane slip
Π	USD/Nm^3	Profit
ρ	kg/m^3	Density
Subscripts		
A	Referent to absorber	
B	Referent to biomethane	
$Burnt$	Referent to the biogas that has to be burnt	
C	Referent to the carbon dioxide stream	
CH_4	Referent to methane	
$Chill$	Referent to chilling system	
D	Referent to desorber	
G	Referent to gas entering absorber	
i	Referent to component i	
L	Referent to liquid entering absorber	
$Lean$	Referent to lean loading	
R	Referent to reboiler	

(continued on next page)

(*continued*)

Symbol	Unit	Meaning
ref	Reference value	
Rich	Referent to rich loading	
S	Referent to solvent	

CRediT authorship contribution statement

Andrés Carranza-Abaid: Conceptualization, Methodology, Software, Validation, Formal analysis, Investigation, Data curation, Writing - original draft, Writing - review & editing, Visualization. **Ricardo R. Wanderley:** Conceptualization, Methodology, Software, Validation, Formal analysis, Investigation, Data curation, Writing - original draft, Writing - review & editing, Visualization. **Hanna K. Knuutila:** Conceptualization, Resources, Supervision, Writing - review & editing, Project administration, Funding acquisition. **Jana Poplsteinova Jakobsen:** Conceptualization, Resources, Supervision, Writing - review & editing, Project administration, Funding acquisition.

Declaration of Competing Interest

The authors declare that they have no known competing financial interests or personal relationships that could have appeared to influence the work reported in this paper.

References

[1] Urban W. Biomethane injection into natural gas networks. In: Wellinger A, Murphy J, Baxter D, editors. Biogas Handb., Woodhead Publishing Limited; 2013, p. 378–403.

[2] Yang F, Meerman JC, Faaij APC. Carbon capture and biomass in industry: a techno-economic analysis and comparison of negative emission options. Renew Sustain Energy Rev 2021;144:111028. https://doi.org/10.1016/j.rser.2021.111028.

[3] Ryckebosch E, Drouillon M, Vervaeren H. Techniques for transformation of biogas to biomethane. Biomass Bioenergy 2011;35(5):1633–45. https://doi.org/10.1016/j.biombioe.2011.02.033.

[4] Petersson A, Wellinger A. Biogas upgrading technologies - developments and innovations. 2009.

[5] Petersson A. Biogas cleaning. In: Wellinger A, Murphy J, Baxter D, editors. Biogas Handb., Woodhead Publishing Limited; 2013, p. 329–41.

[6] Persson M. Evaluation of upgrading techniques for biogas - Rapport SGC 142. 2003.

[7] Weiland P. Biogas production: current state and perspectives. Appl Microbiol Biotechnol 2010;85(4):849–60. https://doi.org/10.1007/s00253-009-2246-7.

[8] Bauer F, Hulteberg C, Persson T, Tamm D. Biogas upgrading - Review of commercial technologies – SGC Rapport 270. 2013.

[9] IEA Bioenergy – Task 37 – Plant Lists 2019. http://task37.ieabioenergy.com/plant-list.html (accessed May 20, 2020).

[10] Nogueira GP, McManus MC, Leak DJ, Franco TT, Oliveira de Souza Dias M, Nakao Cavaliero CK. Are eucalyptus harvest residues a truly burden-free biomass source for bioenergy? A deeper look into biorefinery process design and Life Cycle Assessment. J Clean Prod 2021;299:126956. https://doi.org/10.1016/j.jclepro.2021.126956.

[11] Halliday C, Hatton TA. Net-negative emissions through molten sorbents and bioenergy with carbon capture and storage. Ind Eng Chem Res 2020;59(52):22582–96. https://doi.org/10.1021/acs.iecr.0c0451210.1021/acs.iecr.0c04512.s001.

[12] Bauer F, Persson T, Hulteberg C, Tamm D. Biogas upgrading – technology overview, comparison and perspectives for the future. Biofuels Bioprod Biorefining 2013;7(5):499–511. https://doi.org/10.1002/bbb.2013.7.issue-510.1002/bbb.1423.

[13] Beil M, Beyrich W. Biogas upgrading to biomethane. In: Wellinger A, Murphy J, Baxter D, editors. Biogas Handb., Woodhead Publishing Limited; 2013, p. 342–77.

[14] Niesner J, Jecha D, Stehlík P. Biogas upgrading technologies: state of art review in European Region. Chem Eng Transac 2013;35:517–22. https://doi.org/10.3303/CET1335086.

[15] Hochgesand G. Rectisol and purisol. Ind Eng Chem 1970;62(7):37–43. https://doi.org/10.1021/ie50727a007.

[16] Gamba S, Pellegrini LA. Biogas upgrading: analysis and comparison between water and chemical scrubbings. Chem Eng Trans 2013;32:1273–8.

[17] Riboldi L, Bolland O. Evaluating pressure swing adsorption as a CO2 separation technique in coal-fired power plants. Int J Greenh Gas Control 2015;39:1–16. https://doi.org/10.1016/j.ijggc.2015.02.001.

[18] Zhang Y, Sunarso J, Liu S, Wang R. Current status and development of membranes for CO2/CH4 separation: a review. Int J Greenh Gas Control 2013;12:84–107. https://doi.org/10.1016/j.ijggc.2012.10.009.

[19] Vrbová V, Ciahotný K. Upgrading biogas to biomethane using membrane separation. Energy Fuels 2017;31(9):9393–401. https://doi.org/10.1021/acs.energyfuels.7b00120.

[20] Baena-Moreno FM, Rodríguez-Galán M, Vega F, Vilches LF, Navarrete B, Zhang Z. Biogas upgrading by cryogenic techniques. Environ Chem Lett 2019;17(3):1251–61. https://doi.org/10.1007/s10311-019-00872-2.

[21] Criscuoli A, Drioli E. New metrics for evaluating the performance of membrane operations in the logic of process intensification. Ind. Eng. Chem. Res., vol. 46, American Chemical Society; 2007, p. 2268–71. doi: 10.1021/ie0610952.

[22] Brunetti A, Scura F, Barbieri G, Drioli E. Membrane technologies for CO2 separation. J Memb Sci 2010;359(1-2):115–25. https://doi.org/10.1016/j.memsci.2009.11.040.

[23] Maurya R, Tirkey SR, Rajapitamahuni S, Ghosh A, Mishra S. Recent advances and future prospective of biogas production. Adv. Feed. Convers. Technol. Altern. Fuels Bioprod. New Technol. Challenges Oppor., Elsevier; 2019, p. 159–78. doi: 10.1016/B978-0-12-817937-6.00009-6.

[24] Rochelle GT. Amine scrubbing for CO2 capture. Science (80-) 2009;325(5948):1652–4. https://doi.org/10.1126/science:1176731.

[25] Feron PHM. Absorption-Based Post-combustion Capture of Carbon Dioxide. Elsevier Inc.; 2016. doi: 10.1016/c2014-0-03382-5.

[26] Kapoor R, Ghosh P, Kumar M, Vijay VK. Evaluation of biogas upgrading technologies and future perspectives: a review. Environ Sci Pollut Res 2019;26(12):11631–61. https://doi.org/10.1007/s11356-019-04767-1.

[27] Maggioni L, Pieroni C. Deliverable D5.2: Report on the biomethane injection into national gas grid. 2016.

[28] Prussi M, Julea A, Lonza L, Thiel C. Biomethane as alternative fuel for the EU road sector: analysis of existing and planned infrastructure. Energy Strateg Rev 2021;33:100612. https://doi.org/10.1016/j.esr.2020.100612.

[29] GIIGNL. Position paper on the impact of including methane number in natural gas regulation n.d. https://giignl.org/publications/position-paper-impact-including-methane-number-natural-gas-regulation (accessed April 27, 2021).

[30] Gosiewski K, Pawlaczyk A. Catalytic or thermal reversed flow combustion of coal mine ventilation air methane: What is better choice and when? Chem Eng J 2014;238:78–85. https://doi.org/10.1016/j.cej.2013.07.039.

[31] Moscato I, Munoz DC, Italiano P. Sustainable biomethane: methane slip removal applying regenerative catalytic oxidation (RCO) post combustion technology. Environ Eng Manag J 2020;19:1831–3. https://doi.org/10.30638/eemj.2020.175.

[32] TUV. Biogas to Biomethane Technology Review. 2012.

[33] Lorenzi G, Gorgoroni M, Silva C, Santarelli M. Life cycle assessment of biogas upgrading routes. Energy Procedia, vol. 158, Elsevier Ltd; 2019, p. 2012–8. doi: 10.1016/j.egypro.2019.01.466.

[34] Starr K, Gabarrell X, Villalba G, Talens L, Lombardi L. Life cycle assessment of biogas upgrading technologies. Waste Manag 2012;32(5):991–9. https://doi.org/10.1016/j.wasman.2011.12.016.

[35] Hyatt JA. Liquid and supercritical carbon dioxide as organic solvents. J Org Chem 1984;49(26):5097–101. https://doi.org/10.1021/jo00200a016.

[36] Raveendran P, Wallen SL. Cooperative C-H0 ··· O hydrogen bonding in CO2-Lewis base complexes: implications for solvation in supercritical CO2. J Am Chem Soc 2002;124:12590–9. https://doi.org/10.1021/ja0174635.

[37] Tande B, Seames W, Benson S. Efficient Regeneration of Physical and Chemical Solvents for CO2 Capture. 2013.

[38] Kohl AL, Nielsen RB, Kohl AL, Nielsen RB. Physical solvents for acid gas removal. Gas Purif 1997:1187–237. https://doi.org/10.1016/B978-088415220-0/50014-8.

[39] Gui X, Tang Z, Fei W. Solubility of CO_2 in alcohols, glycols, ethers, and ketones at high pressures from (288.15 to 318.15) K. J Chem Eng Data 2011;56(5):2420–9. https://doi.org/10.1021/je101344v.

[40] Li X, Jiang Y, Han G, Deng D. Investigation of the solubilities of carbon dioxide in some low volatile solvents and their thermodynamic properties. J Chem Eng Data 2016;61(3):1254–61. https://doi.org/10.1021/acs.jced.5b00893.

[41] Aghaie M, Rezaei N, Zendehboudi S. A systematic review on CO2 capture with ionic liquids: current status and future prospects. Renew Sustain Energy Rev 2018;96:502–25. https://doi.org/10.1016/j.rser.2018.07.004.

[42] Enick RM, Koronaios P, Stevenson C, Warman S, Morsi B, Nulwala H, et al. Hydrophobic polymeric solvents for the selective absorption of CO 2 from warm gas streams that also contain H2 and H 2O. Energy Fuels 2013;27(11):6913–20. https://doi.org/10.1021/ef401740w.

[43] Siefert NS, Agarwal S, Shi F, Shi W, Roth EA, Hopkinson D, et al. Hydrophobic physical solvents for pre-combustion CO2 capture: experiments, computational simulations, and techno-economic analysis. Int J Greenh Gas Control 2016;49:364–71. https://doi.org/10.1016/j.ijggc.2016.03.014.

[44] Vega F, Cano M, Camino S, Fernández LMG, Portillo E, Navarrete B. Solvents for carbon dioxide capture. carbon dioxide chem. capture oil recover. InTech 2018. https://doi.org/10.5772/intechopen.71443.

[45] Rackley SA. Absorption capture systems. Carbon Capture and Storage, Elsevier; 2017, p. 115–49. https://doi.org/10.1016/b978-0-12-812041-5.00006-4.

[46] Higman C. Gasification processes and synthesis gas treatment technologies for carbon dioxide (CO2) capture. Dev. Innov. Carbon Dioxide Capture Storage Technol., Elsevier; 2010, p. 243–79. doi: 10.1533/9781845699574.2.243.

[47] Burr B, Lyddon L. A comparison of physical solvents for acid gas removal. Digit Refin 2008. https://www.digitalrefining.com/article/1000560#.XqE2B8gzZPY (accessed April 23, 2020).

[48] Nagaraju Palla, Dennis Leppin. Technical and Operating Support for Pilot Demonstration of Morphysorb Acid Gas Removal Process. Pittsburgh, PA, and Morgantown, WV: 2003. doi: 10.2172/822134.

[49] Boll W, Hochgesand G, Higman C, Supp E, Kalteier P, Müller W-D, et al. Gas Production, 3. Gas Treating. Ullmann's Encycl. Ind. Chem., Weinheim, Germany: Wiley-VCH Verlag GmbH & Co. KGaA; 2011. doi: 10.1002/14356007.o12_o02.

[50] Bucklin RW, Schendel RL. Comparison of Physical Solvents Used for Gas Processing. In: Newman SA, editor. Acid Sour Gas Treat. Process., 1985, p. 42–79.

[51] Bhattacharyya D, Turton R, Zitney SE. Acid gas removal from syngas in IGCC plants. Integr. Gasif. Comb. Cycle Technol., Elsevier Inc.; 2017, p. 385–418. https://doi.org/10.1016/B978-0-08-100167-7.00011-1.

[52] Bell DA, Towler BF, Fan M. Sulfur Recovery. Coal Gasif. Its Appl., William Andrew Publishing; 2010, p. 113–36. doi: 10.1016/B978-0-8155-2049-8.10006-3.

[53] Rayer AV, Henni A, Tontiwachwuthikul P. High pressure physical solubility of carbon dioxide (CO2) in mixed polyethylene glycol dimethyl ethers (Genosorb 1753). Can J Chem Eng 2012;90(3):576–83. https://doi.org/10.1002/cjce.20615.

[54] Ordorica-Garcia JG, Elkamel A, Douglas PL, Croiset E. Clean-Coal Technology: Gasification Pathway. Environ. Conscious Foss. Energy Prod., Hoboken, NJ, USA: John Wiley & Sons, Inc.; 2009, p. 243–76. doi: 10.1002/9780470432747.ch7.

[55] Bucklin RW, Schendel RL. Comparison of fluor solvent and selexol processes. Energy Prog 1984;4:137–42.

[56] Isaacs EE, Otto FD, Mather AE. Solubility of hydrogen sulfide and carbon dioxide in a Sulfinol solution. J Chem Eng Data 1977;22(3):317–9. https://doi.org/10.1021/je60074a024.

[57] Ghanbarabadi H, Khoshandam B, Wood DA. Simulation of CO2 removal from ethane with Sulfinol-M+AMP solvent instead of DEA solvent in the South Pars phases 9 and 10 gas processing facility. Petroleum 2019;5(1):90–101. https://doi.org/10.1016/j.petlm.2018.06.004.

[58] Yih S-M, Lai H-C. Simultaneous absorption of CO2 and H2S in sulfinol solutions in a set of packed absorber-stripper. Chem Eng Commun 1990;88:119–25. https://doi.org/10.1080/00986449008940551.

[59] Décultot M, Ledoux A, Fournier-Salaün MC, Estel L. Solubility of CO2 in methanol, ethanol, 1,2-propanediol and glycerol from 283.15 K to 373.15 K and up to 6.0 MPa. J Chem Thermodyn 2019;138:67–77. https://doi.org/10.1016/j.jct.2019.05.003.

[60] Lyu Z, Ma H, Zhang H, Ying W. Solubility of carbon dioxide in methanol from 213.15 K to 273.15 K: Measurement and modeling. Fluid Phase Equilib 2018;471:40–54. https://doi.org/10.1016/j.fluid.2018.04.014.

[61] Xia J, Jödecke M, Kamps APS, Maurer G. Solubility of CO2 in (CH3OH + H2O). J Chem Eng Data 2004;49(6):1756–9. https://doi.org/10.1021/je049803i.

[62] Jou FY, Deshmukh RD, Otto FD, Mather AE. Solubility of H2S, CO2 and CH4 in N-formyl morpholine. J Chem Soc Faraday Trans 1 Phys Chem Condens Phases 1989;85:2675–82. https://doi.org/10.1039/F19898502675.

[63] Xu Y, Schutte RP, Hepler LG. Solubilities of carbon dioxide, hydrogen sulfide and sulfur dioxide in physical solvents. Can J Chem Eng 1992;70(3):569–73. https://doi.org/10.1002/cjce:v70:310.1002/cjce:5450700321.

[64] Murrieta-Guevara F, Romero-Martinez A, Trejo A. Solubilities of carbon dioxide and hydrogen sulfide in propylene carbonate, N-methylpyrrolidone and sulfolane. Fluid Phase Equilib 1988;44(1):105–15. https://doi.org/10.1016/0378-3812(88)80106-7.

[65] Murrieta-Guevara F, Trejo Rodriguez A. Solubility of carbon dioxide, hydrogen sulfide, and methane in pure and mixed solvents. J Chem Eng Data 1984;29(4):456–60. https://doi.org/10.1021/je00038a027.

[66] Bohloul MR, Vatani A, Peyghambarzadeh SM. Experimental and theoretical study of CO2 solubility in N-methyl-2-pyrrolidone (NMP). Fluid Phase Equilib 2014;365:106–11. https://doi.org/10.1016/j.fluid.2013.12.019.

[67] Melzer WM, Schrödter F, Knapp H. Solubilities of methane, propane and carbon dioxide in solvent mixtures consisting of water, N, N-dimethylformamide, and N-methyl-2-pyrrolidone. Fluid Phase Equilib 1989;49:167–86. https://doi.org/10.1016/0378-3812(89)80014-7.

[68] Li Y, Liu Q, Huang W, Yang J. Below the room temperature measurements of solubilities in ester absorbents for CO2 capture. J Chem Thermodyn 2018;127:71–9. https://doi.org/10.1016/j.jct.2018.07.021.

[69] Thompson R, Culp JT, Tiwari SP, Shi W, Siefert N, Hopkinson DP. CO2 Solubility in Organophosphate Physical Solvents Wherein Alkyl Groups Are Replaced with Poly(Ethylene Glycol) Groups 2019. doi: 10.26434/CHEMRXIV.11348051.V1.

[70] Jou FY, Deshmukh RD, Otto FD, Mather AE. Solubility of H2S, CO2, CH4 and C2H6 in sulfolane at elevated pressures. Fluid Phase Equilib 1990;56:313–24. https://doi.org/10.1016/0378-3812(90)85111-M.

[71] Schnabel T, Vrabec J, Hasse H. Molecular simulation study of hydrogen bonding mixtures and new molecular models for mono- and dimethylamine. Fluid Phase Equilib 2008;263(2):144–59. https://doi.org/10.1016/j.fluid.2007.10.003.

[72] Kapateh MH, Chapoy A, Burgass R, Tohidi B. Experimental measurement and modeling of the solubility of methane in methanol and ethanol. J Chem Eng Data 2016;61(1):666–73. https://doi.org/10.1021/acs.jced.5b00793.

[73] Frost M, Karakatsani E, Von Solms N, Richon D, Kontogeorgis GM. Vapor-liquid equilibrium of methane with water and methanol. Measurements and modeling. J Chem Eng Data 2014;59(4):961–7. https://doi.org/10.1021/je400684k.

[74] Henni A, Tontiwachwuthikul P, Chakma A. Solubility Study of Methane and Ethane in Promising Physical Solvents for Natural Gas Sweetening Operations 2006. doi: 10.1021/je050172h.

[75] Jou F-Y, Mather AE, Schmidt KAG. Solubility of methane in propylene carbonate. J Chem Eng Data 2015;60(4):1010–3. https://doi.org/10.1021/je500849m.

[76] Rayer AV, Henni A, Tontiwachwuthikul P. High-pressure solubility of methane (CH 4) and ethane (C 2H 6) in mixed polyethylene glycol dimethyl ethers (Genosorb 1753) and its selectivity in natural gas sweetening operations. J Chem Eng Data 2012;57(3):764–75. https://doi.org/10.1021/je200905z.

[77] Rajasingam R, Lioe L, Pham QT, Lucien FP. Solubility of carbon dioxide in dimethylsulfoxide and N-methyl-2-pyrrolidone at elevated pressure. J Supercrit Fluids 2004;31(3):227–34. https://doi.org/10.1016/j.supflu.2003.12.003.

[78] Chen H, Li HQ, Tu WX, Bao WJ, Li SP. Measurement of CO2 solubility in tributyl phosphate. Guocheng Gongcheng Xuebao/The Chinese J Process Eng 2012;12:206–11.

[79] Shi W, Thompson RL, Macala MK, Resnik K, Steckel JA, Siefert NS, et al. Molecular Simulations of CO2 and H2 Solubility, CO2 Diffusivity, and Solvent Viscosity at 298 K for 27 Commercially Available Physical Solvents. J Chem Eng Data 2019;64:3682–92. doi: 10.1021/acs.jced.8b01228.

[80] Svensson H, Zejnullahu Velasco V, Hulteberg C, Karlsson HT. Heat of absorption of carbon dioxide in mixtures of 2-amino-2-methyl-1-propanol and organic solvents. Int J Greenh Gas Control 2014;30:1–8. https://doi.org/10.1016/J.IJGGC.2014.08.022.

[81] Wanderley RR, Evjen S, Pinto DDD, Knuutila HK. The salting-out effect in some physical absorbents for CO2 capture. Chem Eng Trans 2018;69:97–102. https://doi.org/10.3303/CET1869017.

[82] Dodds WS, Stutzman LF, Sollami BJ. Carbon dioxide solubility in water. Ind Eng Chem – Chem Eng Data Ser 1956;1(1):92–5. https://doi.org/10.1021/i460001a018.

[83] Diamond LW, Akinfiev NN. Solubility of CO2 in water from -1.5 to 100°C and from 0.1 to 100 MPa: evaluation of literature data and thermodynamic modelling. Fluid Phase Equilib 2003;208(1-2):265–90. https://doi.org/10.1016/S0378-3812(03)00041-4.

[84] Lucile F, Cézac P, Contamine F, Serin JP, Houssin D, Arpentinier P. Solubility of carbon dioxide in water and aqueous solution containing sodium hydroxide at temperatures from (293.15 to 393.15) K and pressure up to 5 MPa: experimental measurements. J Chem Eng Data 2012;57(3):784–9. https://doi.org/10.1021/je200991x.

[85] Chapoy A, Mohammadi AH, Chareton A, Tohidi B, Richon D. Measurement and modeling of gas solubility and literature review of the properties for the carbon dioxide-water system. Ind Eng Chem Res 2004;43(7):1794–802. https://doi.org/10.1021/ie034232t.

[86] Dalmolin I, Skovroinski E, Biasi A, Corazza ML, Dariva C, Oliveira J Vladimir. Solubility of carbon dioxide in binary and ternary mixtures with ethanol and water. Fluid Phase Equilib 2006;245(2):193–200. https://doi.org/10.1016/j.fluid.2006.04.017.

[87] Valtz A, Chapoy A, Coquelet C, Paricaud P, Richon D. Vapour-liquid equilibria in the carbon dioxide-water system, measurement and modelling from 278.2 to 318.2 K. Fluid Phase Equilib 2004;226:333–44. https://doi.org/10.1016/j.fluid.2004.10.013.

[88] Servio P, Englezos P. Measurement of dissolved methane in water in equilibrium with its hydrate. J Chem Eng Data 2002;47(1):87–90. https://doi.org/10.1021/je0102255.

[89] Culberson OL, McKetta JJ. Phase equilibria in hydrocarbon-water systems III – The solubility of methane in water at pressures to 10,000 PSIA. J Pet Technol 1951;3:223–6. https://doi.org/10.2118/951223-g.

[90] Clever HL, Young CL, Battino R, Hayduk W, Wiesenburg DA. Methane. Pergamon; 1987.

[91] Lekvam K, Raj Bishnoi P. Dissolution of methane in water at low temperatures and intermediate pressures. Fluid Phase Equilib 1997;131(1-2):297–309. https://doi.org/10.1016/S0378-3812(96)03229-3.

[92] Abatzoglou N, Boivin S. A review of biogas purification processes. Biofuels, Bioprod Biorefining 2009;3(1):42–71. https://doi.org/10.1002/bbb.v3:110.1002/bbb.117.

[93] Rochelle GT. Conventional amine scrubbing for CO2 capture. Absorption-Based Post-Combustion Capture of Carbon Dioxide, Elsevier Inc.; 2016, p. 35–67. doi: 10.1016/B978-0-08-100514-9.00003-2.

[94] Kohl AL, Nielsen RB, Kohl AL, Nielsen RB. Alkanolamines for hydrogen sulfide and carbon dioxide removal. Gas Purif 1997:40–186. https://doi.org/10.1016/B978-088415220-0/50002-1.

[95] Yuan Y, Rochelle GT. Lost work: A comparison of water-lean solvent to a second generation aqueous amine process for CO 2 capture. Int J Greenh Gas Control 2019;84:82–90. https://doi.org/10.1016/j.ijggc.2019.03.013.

[96] Vega F, Sanna A, Navarrete B, Maroto-Valer MM, Cortés VJ. Degradation of amine-based solvents in CO2 capture process by chemical absorption. Greenh Gases Sci Technol 2014;4(6):707–33. https://doi.org/10.1002/ghg.2014.4.issue-610.1002/ghg.1446.

[97] Krzemień A, Wieckol-Ryk A, Smoliński A, Koteras A, Wiecław-Solny L. Assessing the risk of corrosion in amine-based CO2 capture process. J Loss Prev Process Ind 2016;43:189–97. https://doi.org/10.1016/j.jlp.2016.05.020.

[98] Karl M, Castell N, Simpson D, Solberg S, Starrfelt J, Svendby T, et al. Uncertainties in assessing the environmental impact of amine emissions from a CO2 capture plant. Atmos Chem Phys 2014;14:8533–57. https://doi.org/10.5194/acp-14-8533-2014.

[99] Azzi M, White S. Emissions from amine-based post-combustion CO2 capture plants. Absorption-Based Post-Combustion Capture of Carbon Dioxide, Elsevier Inc.; 2016, p. 488–504. doi: 10.1016/B978-0-08-100514-9.00020-2.

[100] Gjernes E, Helgesen LI, Maree Y. Health and environmental impact of amine based post combustion CO 2 capture. Energy Procedia, vol. 37, Elsevier Ltd; 2013, p. 735–42. doi: 10.1016/j.egypro.2013.05.162.

[101] Lepaumier H, Da Silva EF, Einbu A, Grimstvedt A, Knudsen JN, Zahlsen K, et al. Comparison of MEA degradation in pilot-scale with lab-scale experiments. Energy Procedia, vol. 4, Elsevier Ltd; 2011, p. 1652–9. doi: 10.1016/j.egypro.2011.02.037.
[102] Bernhardsen IM, Knuutila HK. A review of potential amine solvents for CO2 absorption process: absorption capacity, cyclic capacity and pKa. Int J Greenh Gas Control 2017;61:27–48. https://doi.org/10.1016/J.IJGGC.2017.03.021.
[103] Conway W, Bruggink S, Beyad Y, Luo W, Melián-Cabrera I, Puxty G, et al. CO2 absorption into aqueous amine blended solutions containing monoethanolamine (MEA), N, N-dimethylethanolamine (DMEA), N, N-diethylethanolamine (DEEA) and 2-amino-2-methyl-1-propanol (AMP) for post-combustion capture processes. Chem Eng Sci 2015;126:446–54. https://doi.org/10.1016/j.ces.2014.12.053.
[104] Conway W, Beyad Y, Feron P, Richner G, Puxty G. CO2 absorption into aqueous amine blends containing benzylamine (BZA), monoethanolamine (MEA), and sterically hindered / tertiary amines. Energy Procedia, vol. 63, Elsevier Ltd; 2014, p. 1835–41. doi: 10.1016/j.egypro.2014.11.191.
[105] Wanderley RR, Pinto DDD, Knuutila HK. From hybrid solvents to water-lean solvents – a critical and historical review. Sep Purif Technol 2021;260:118193. https://doi.org/10.1016/j.seppur.2020.118193.
[106] Sanchez-Fernandez E, Heffernan K, Van Der Ham L, Linders MJG, Goetheer ELV, Vlugt TJH. Precipitating amino acid solvents for CO2 capture. Opportunities to reduce costs in Post combustion capture. Energy Procedia, vol. 63, Elsevier Ltd; 2014, p. 727–38. doi: 10.1016/j.egypro.2014.11.080.
[107] Moioli S, Pellegrini LA, Ho MT, Wiley DE. A comparison between amino acid based solvent and traditional amine solvent processes for CO2 removal. Chem Eng Res Des 2019;146:509–17. https://doi.org/10.1016/j.cherd.2019.04.035.
[108] Pinto DDD, Knuutila H, Fytianos G, Haugen G, Mejdell T, Svendsen HF. CO2 post combustion capture with a phase change solvent. Pilot plant campaign. Int J Greenh Gas Control 2014;31:153–64. https://doi.org/10.1016/j.ijggc.2014.10.007.
[109] Sanchez Fernandez E, Heffernan K, Van Der Ham LV, Linders MJG, Eggink E, Schrama FNH, et al. Conceptual design of a novel CO2 capture process based on precipitating amino acid solvents. Ind Eng Chem Res 2013;52(34):12223–35. https://doi.org/10.1021/ie401228r.
[110] Rochelle G, Chen E, Freeman S, Van Wagener D, Xu Q, Voice A. Aqueous piperazine as the new standard for CO2 capture technology. Chem Eng J 2011;171(3):725–33.
[111] Feron PHM, Cousins A, Jiang K, Zhai R, Garcia M. An update of the benchmark post-combustion CO2-capture technology. Fuel 2020;273:117776. https://doi.org/10.1016/j.fuel.2020.117776.
[112] Lee WY, Park SY, Lee KB, Nam SC. Simultaneous removal of CO2 and H2S from biogas by blending amine absorbents: a performance comparison study. Energy Fuels 2020;34(2):1992–2000. https://doi.org/10.1021/acs.energyfuels.9b03342.
[113] Capra F, Fettarappa F, Magli F, Gatti M, Martelli E. Biogas upgrading by amine scrubbing: Solvent comparison between MDEA and MDEA/MEA blend. Energy Procedia, vol. 148, Elsevier Ltd; 2018, p. 970–7. doi: 10.1016/j.egypro.2018.08.065.
[114] Privalova EI, Mäki-Arvela P, Eränen K, Avetisov AK, Mikkola J-P, Murzin D Yu. Amine solutions for biogas upgrading: ideal versus non-ideal absorption isotherms. Chem Eng Technol 2013;36(5):740–8. https://doi.org/10.1002/ceat.v36.510.1002/ceat.201200161.
[115] Costa C, Demartini M, Di Felice R, Oliva M, Pagliai P. Piperazine and methyldiethanolamine interrelationships in CO2 absorption by aqueous amine mixtures. Part I: Saturation rates of single-reagent solutions. Can J Chem Eng 2019;97(5):1160–71. https://doi.org/10.1002/cjce:v97.510.1002/cjce:23320.
[116] Abdeen FRH, Mel M, Jami MS, Ihsan SI, Ismail AF. A review of chemical absorption of carbon dioxide for biogas upgrading. Chinese J Chem Eng 2016;24(6):693–702. https://doi.org/10.1016/j.cjche.2016.05.006.
[117] Closmann F, Nguyen T, Rochelle GT. MDEA/Piperazine as a solvent for CO2 capture. Energy Procedia, vol. 1, Elsevier; 2009, p. 1351–7. doi: 10.1016/j.egypro.2009.01.177.
[118] Kim I, Svendsen HF. Heat of absorption of carbon dioxide (CO2) in monoethanolamine (MEA) and 2-(aminoethyl)ethanolamine (AEEA) solutions. Ind Eng Chem Res 2007;46(17):5803–9. https://doi.org/10.1021/ie0616489.
[119] Svendsen HF, Hessen ET, Mejdell T. Carbon dioxide capture by absorption, challenges and possibilities. Chem Eng J 2011;171(3):718–24. https://doi.org/10.1016/j.cej.2011.01.014.
[120] Kim I, Hoff KA, Mejdell T. Heat of absorption of CO2 with aqueous solutions of MEA: New experimental data. Energy Procedia 2014;63:1446–55. https://doi.org/10.1016/j.egypro.2014.11.154.
[121] Aronu UE, Gondal S, Hessen ET, Haug-Warberg T, Hartono A, Hoff KA, et al. Solubility of CO2 in 15, 30, 45 and 60 mass% MEA from 40 to 120 °C and model representation using the extended UNIQUAC framework. Chem Eng Sci 2011;66(24):6393–406.
[122] Carranza-Abaid A, Svendsen HF, Jakobsen JP. Surrogate modelling of VLE: integrating machine learning with thermodynamic constraints. Chem Eng Sci X 2020;8:100080. https://doi.org/10.1016/j.cesx.2020.100080.
[123] Gabrielsen J, Michelsen ML, Stenby EH, Kontogeorgis GM. A model for estimating CO2 solubility in aqueous alkanolamines. Ind Eng Chem Res 2005;44(9):3348–54. https://doi.org/10.1021/ie048857i.
[124] Moioli S, Pellegrini LA. Modeling the methyldiethanolamine-piperazine scrubbing system for CO2 removal: Thermodynamic analysis. Front Chem Sci Eng 2016;10(1):162–75. https://doi.org/10.1007/s11705-016-1555-5.
[125] Øi LE, Brathen T, Berg C, Brekne SK, Flatin M, Johnsen R, et al. Optimization of configurations for amine based CO2 absorption using Aspen HYSYS. Energy Procedia, vol. 51, Elsevier Ltd; 2014, p. 224–33. doi: 10.1016/j.egypro.2014.07.026.
[126] Beil M, Beyrich W. Biogas upgrading to biomethane. 2013. doi: 10.1533/9780857097415.3.342.
[127] Budzianowski WM, Wylock CE, Marciniak PA. Power requirements of biogas upgrading by water scrubbing and biomethane compression: Comparative analysis of various plant configurations. Energy Convers Manag 2017;141:2–19. https://doi.org/10.1016/j.enconman.2016.03.018.
[128] Masson-Delmotte V, Pörtner H-O, Skea J. IPCC report Global Warming of 1.5 °C. 2018.
[129] Lombardi L, Francini G. Techno-economic and environmental assessment of the main biogas upgrading technologies. Renew Energy 2020;156:440–58. https://doi.org/10.1016/j.renene.2020.04.083.
[130] Smith R. Chemical Process Design and Integration. 2nd ed. McGraw-Hill; 2005. doi: 10.1529/biophysj.107.124164.
[131] Tobiesen FA, Svendsen HF, Juliussen O. Experimental Validation of a Rigorous Absorber Model for CO2 Postcombustion Capture 2007;53. doi: 10.1002/aic.
[132] Faramarzi L, Kontogeorgis GM, Michelsen ML, Thomsen K, Stenby EH. Absorber Model for CO2 Capture by Monoethanolamine 2010:3751–9. doi: 10.1021/ie901671f.
[133] Carranza-Abaid A, Jakobsen JP. A Non-Autonomous Relativistic Frame of Reference for Unit Operation Design. vol. 48. 2020. doi: 10.1016/B978-0-12-823377-1.50026-4.
[134] Kvamsdal HM, Rochelle GT. Effects of the Temperature Bulge in CO 2 Absorption from Flue Gas by Aqueous Monoethanolamine 2008. doi: 10.1021/ie061651s.
[135] Cousins A, Cottrell A, Lawson A, Huang S, Feron PHM. Model verification and evaluation of the rich-split process modification at an Australian-based post combustion CO 2 capture pilot plant. Greenh Gases Sci Technol 2012;2(5):329–45. https://doi.org/10.1002/ghg.v2.510.1002/ghg.1295.
[136] Smith JM, Van Ness HC, MMA. Introduction to Chemical Engineering Thermodynamics. 3rd ed. McGraw-Hill, Inc.; 2004.
[137] Stewart M, Mcguire R, White R. Surface Production Operations: Design of Oil-Handling Systems and Facilities. Elsevier; 1999. doi: 10.1016/B978-0-88415-821-9.X5000-3.
[138] Bellos E, Tzivanidis C. A comparative study of CO2 refrigeration systems. Energy Convers Manag X 2019;1:100002. https://doi.org/10.1016/j.ecmx.2018.100002.
[139] International Organization for Standarization. ISO 14008: 2019—Monetary Valuation of Environmental Impacts and Related Environmental Aspects. 2019.
[140] Methanol Price and Supply/Demand 2021.
[141] Campbell JM. Gas Conditioning and Processing, Vol. 2: The Equipment Modules. 9th ed. Norman, Oklahoma: Campbell Petroleum Series; 2014.
[142] Henry hub natural gas spot price 2019.
[143] Statista. Average retail electricity price for industrial consumers in the U.S. from 1970 to 2019 2019.
[144] Zapiain-Salinas JG, Barajas-Fernández J, González-García R. Modified method to improve the design of Petlyuk distillation columns. Chem Cent J 2014;8:2–11. https://doi.org/10.1186/1752-153X-8-41.
[145] Mokhatab S, Poe WA, Mak JY. Natural Gas Treating. 2019. doi: 10.1016/b978-0-12-815817-3.00007-1.
[146] Conesa A, Shen S, Coronas A. Liquid densities, kinematic viscosities, and heat capacities of some ethylene glycol dimethyl ethers at temperatures from 283.15 to 423.15 K. Int J Thermophys 1998;19:1343–58. https://doi.org/10.1023/A:1021927417610.
[147] Langan JR, Salmon GA. Physical properties of N-methylpyrrolidinone as functions of temperature. J Chem Eng Data 1987;32(4):420–2. https://doi.org/10.1021/je00050a009.
[148] Xiang HW, Laesecke A, Huber ML. A new reference correlation for the viscosity of methanol. J Phys Chem Ref Data 2006;35(4):1597–620. https://doi.org/10.1063/1.2360605.
[149] Korson L, Drost-Hansen W, Millero FJ. Viscosity of water at various temperatures. J Phys Chem 1969;73(1):34–9. https://doi.org/10.1021/j100721a006.
[150] Moser P, Wiechers G, Schmidt S, Goetheer E, Garcia J, Monteiro M, et al. ALIGN-CCUS: results of the 18-month test with MEA at the pilot plant at Niederaussem – solvent management, emissions and dynamic behavior. IEAGHG 5th Post Combust Capture Conf 2019:1–7.
[151] Seader JD, Henley EJ. Separation process principles. 2nd ed. Wiley Series; 2004.
[152] Panahi H, Eslami A, Golozar MA, Ashrafi Laleh A, Aryanpur M, Mazarei M. Failure analysis of type 304 stainless steel amine exchanger sheets in a gas sweetening plant. Case Stud Eng Fail Anal 2017;9:87–98. https://doi.org/10.1016/j.csefa.2017.08.002.
[153] Wu X, Wang M, Liao P, Shen J, Li Y. Solvent-based post-combustion CO2 capture for power plants: a critical review and perspective on dynamic modelling, system identification, process control and flexible operation. Appl Energy 2020;257:113941. https://doi.org/10.1016/j.apenergy.2019.113941.